Cooperative stochastic MPC under hard input constraints and event-triggered communication

Irene Perez-Salesa, *Graduate Student Member, IEEE*, Dimos V. Dimarogonas, *Fellow, IEEE*, Carlos Sagüés, *Senior Member, IEEE*, Rodrigo Aldana-López, *Member, IEEE*

***Abstract*—In this work, we develop a new distributed output-feedback stochastic model predictive control (SMPC) proposal for a plant that is cooperatively regulated by a set of actuator nodes. Contrary to most approaches, we consider hard constraints on the actuators, and we appropriately tighten the constraints to ensure recursive feasibility with a given probability, despite the stochastic noise present in the system. To lighten the communication load, the constraint design is performed offline and an event-triggering mechanism is included, so that the nodes only need to transmit their local state estimates to neighbors at event instants during online execution. We prove constraint satisfaction and stability of our proposal, and we include simulation results showing that similar control performance to the centralized case can be achieved by our distributed SMPC with reduced communication.**

***Index Terms*—Constrained control, cooperative model predictive control, stochastic systems.**

I. Introduction

Stochastic model predictive control (SMPC) has been studied as an alternative to robust MPC when a probabilistic characterization of the disturbances in the system is available. SMPC takes into account the probability distribution of the disturbance rather than considering its worst-case bounds. In addition, chance constraints are considered, allowing a certain probability of constraint violation, which results in a less conservative approach than considering hard constraints. SMPC finds applications in fields such as networked and industrial process control, building climate regulation, robotic path planning and cooperative transportation [1]. Analogous to robust MPC techniques, a popular approach to SMPC is to perform a deterministic reformulation of the problem, by appropriately tightening the constraints around the nominal trajectory of the system, taking into account the probability distribution of disturbances. Then, the controller solves the optimization considering only the undisturbed trajectory, so that standard MPC solutions can be applied.

The centralized SMPC problem has been widely addressed in the literature. The linear and state feedback case is tackled in [2], [3], while output-feedback is considered in [4]–[8]. Nonlinear systems with output-feedback have been addressed in [9], [10]. To reduce the computational load of solving the optimization problem at each time step, event and self-triggered approaches have also been developed to decide when to recompute the control input [11]–[14], with appropriate triggering conditions that ensure stability and recursive feasibility of the optimization problem.

Distributed SMPC schemes have also been developed for multi-agent and large-scale systems, where each of the actuator agents must consider neighbor data to perform the desired task, due to couplings in the system's dynamics, constraints or in the shared control objective. In [15], subsystems of a large-scale plant with coupled state dynamics compute their local control inputs in a distributed fashion by solving local optimization problems. In [16], a distributed optimization algorithm is used to compute inputs, and the effect of inexact minimization is studied. In [17], a data-driven controller is proposed, while [18] addresses the case with delays. The proposals from [19], [20] consider agents with uncoupled dynamics but coupled probabilistic constraints, in environments such as vehicle platooning. These two works also include event and self-triggered mechanisms to reduce the communication load between the agents. Despite several works addressing distributed SMPC, most proposals are limited to state feedback. For the case with output-feedback, [21] considers a similar setup to [19], [20], while [22] proposes an output-feedback scheme for systems with coupled dynamics using probabilistic reachable sets. To construct these sets for constraint tightening in the distributed case, neighbor information needs to be taken into account. Here, the computation of tightened constraints and control inputs is solved via distributed optimization, which requires high communication rates. In addition, chance input constraints are considered in the previous distributed SMPC works, which may be unrealistic for the actuators in practice.

In this work, we focus on distributed output-feedback stochastic control of a plant that is cooperatively regulated by several actuator nodes. We consider practical issues such as noisy sensor data, input saturation and communication

Manuscript submitted on 21 May, 2025. This work was supported via projects PID2021-124137OB-I00 and TED2021-130224B-I00 funded by MCIN/AEI/10.13039/501100011033, by ERDF A way of making Europe and by the European Union NextGenerationEU/PRTR, by the Gobierno de Aragón under Project DGA T45-23R, by the Universidad de Zaragoza and by Spanish grants FPU20/03134 and EST24/00112.

I. Perez-Salesa, C. Sagüés and R. Aldana-López are with Departamento de Informatica e Ingenieria de Sistemas (DIIS) and Instituto de Investigacion en Ingenieria de Aragon (I3A), Universidad de Zaragoza, Maria de Luna 1, 50018 Zaragoza, Spain (e-mails: i.perez@unizar.es, csagues@unizar.es, rodrigo.aldana.lopez@gmail.com).

D. V. Dimarogonas is with Division of Decision and Control Systems, School of Electrical Engineering and Computer Science, KTH Royal Institute of Technology, SE-100 44, Stockholm, Sweden (e-mail: dimos@kth.se).

limitations in the system, extending the theoretical SMPC formulations in the literature to explicitly address these problems. Our contributions are the following: 1) We propose an SMPC scheme under mixed constraints, which accounts for the stochastic disturbances and the hard input saturations, in contrast to prior distributed SMPC works. Our proposal relies on a consensus-based event-triggered distributed state estimator to handle noisy sensor data while coordinating the information at the actuator nodes, as an alternative to communication-intensive distributed optimization approaches. Each node exchanges only its state estimate with neighbors at sparse event instants, and computes its control input via a local optimization problem using its own estimate. 2) We design tightened constraints to ensure constraint satisfaction, as well as recursive feasibility of the optimization problem with no less than a user-defined probability, which can be lost due to the mixed constraints. We take a similar approach to [6], which addresses centralized SMPC with hard input constraints; however, due to our distributed setup, the effects of neighbor information, limited communication and coupled dynamics need to be taken into account. We extend such analysis and design to the distributed case. Moreover, our constraints are tightened offline to further reduce communication. 3) We include formal analysis of the recursive feasibility, constraint satisfaction and stability of our proposal, as well as simulation experiments to validate our results.

A. Notation

The $n \times n$ identity matrix is denoted by $\mathbf{I}_n$ and the $n \times 1$ vector of ones is $\mathbb{1}_n$. The operators $\mathbb{P}\{\bullet\}$, $\mathbb{E}\{\bullet\}$ and $\mathsf{cov}\{\bullet\}$ denote probability measure, expectation and covariance. $\|\bullet\|$ represents the Euclidean norm and induced norm when applied to a vector or a matrix, respectively, with $\|\mathbf{x}\|_{\mathbf{P}}^2 = \mathbf{x}^\top \mathbf{P}\mathbf{x}$ for a vector $\mathbf{x}$ and matrix $\mathbf{P}$. The Kronecker product is $\otimes$, the Minkowski sum is $\oplus$ and the Pontryagin difference is $\ominus$. The notation $\bigoplus_{i=0}^{N}$ denotes the Minkowski sum of N sets indexed by i. For two polytopes $\mathcal{P}_1 \subseteq \mathbb{R}^{p_1}$, $\mathcal{P}_2 \subseteq \mathbb{R}^{p_2}$, their product is $\mathcal{P}_1 \times \mathcal{P}_2 = \{[\mathbf{x}_1, \mathbf{x}_2] : \mathbf{x}_1 \in \mathcal{P}_1,\ \mathbf{x}_2 \in \mathcal{P}_2\} \subseteq \mathbb{R}^{p_1+p_2}$. $\lambda_{\max}(\bullet)$ is the maximum eigenvalue of a matrix. The normal distribution with mean $\boldsymbol{\mu}$ and covariance $\boldsymbol{\Sigma}$ is given by $\mathcal{N}(\boldsymbol{\mu}, \boldsymbol{\Sigma})$. $\mathbf{A} \succ \mathbf{0}$ ($\mathbf{A} \succeq \mathbf{0}$) implies that $\mathbf{A}$ is positive definite (semidefinite). For vectors, we use $\geq, \leq$ for element-wise comparison. The notations $\mathsf{row}_{i=1}^{N}(\bullet_i)$, $\mathsf{col}_{i=1}^{N}(\bullet_i)$ and $\mathsf{diag}_{i=1}^{N}(\bullet_i)$ for some matrices indexed with $i = 1, \dots, N$ are their row, column and block-diagonal compositions. The notation $[\bullet]_m$ denotes the mth component (row) if applied to a vector (matrix). The notation $\because$ means "because". $\mathbb{Z}_{\geq 0}$ denotes non-negative integers.

II. Problem Statement

We consider a plant cooperatively regulated by a set of N actuator nodes, with dynamics described by

$$\dot{\mathbf{x}}(t) = \mathbf{A}\mathbf{x}(t) + \textstyle\sum_{i=1}^{N} \mathbf{B}_i \mathbf{u}_i(t) + \mathbf{w}(t), \tag{1a}$$

$$\mathbf{y}_i(t) = \mathbf{C}_i \mathbf{x}(t) + \mathbf{v}_i(t), \tag{1b}$$

where $\mathbf{x}(t) \in \mathbb{R}^{n_{\mathbf{x}}}$ is the state of the plant, $\mathbf{u}_i(t) \in \mathbb{R}^{n_{\mathbf{u},i}}$ is the control input from the ith actuator node, $\mathbf{y}_i(t)$ is the local measurement available to the ith actuator node, and $\mathbf{w}(t)$, $\mathbf{v}_i(t)$ are stochastic disturbances, representing disturbances to the plant and the local measurement noises, respectively.

The global system dynamics can be equivalently described in a compact form by

$$\begin{aligned} \dot{\mathbf{x}}(t) &= \mathbf{A}\mathbf{x}(t) + \mathbf{B}\mathbf{u}(t) + \mathbf{w}(t), \\ \mathbf{y}(t) &= \mathbf{C}\mathbf{x}(t) + \mathbf{v}(t), \end{aligned} \tag{2}$$

by defining $\mathbf{u}(t) = \mathsf{col}_{i=1}^{N}(\mathbf{u}_i(t)) \in \mathbb{R}^{n_{\mathbf{u}}}$, $\mathbf{y}(t) = \mathsf{col}_{i=1}^{N}(\mathbf{y}_i(t))$, $\mathbf{v}(t) = \mathsf{col}_{i=1}^{N}(\mathbf{v}_i(t))$, $\mathbf{B} = \mathsf{row}_{i=1}^{N}(\mathbf{B}_i)$ and $\mathbf{C} = \mathsf{col}_{i=1}^{N}(\mathbf{C}_i)$. The initial state is $\mathbf{x}(0) \sim \mathcal{N}(\mathbf{x}_0, \mathbf{P}_0)$, with mean $\mathbf{x}_0$ and covariance $\mathbf{P}_0$.

Assumption 1: The global pairs $(\mathbf{A}, \mathbf{B})$ and $(\mathbf{A}, \mathbf{C})$ in (2) are controllable and observable, respectively.

Assumption 2: The stochastic disturbance $\mathbf{w}(t)$ in (1a) follows $\mathbf{w}(t) \sim \mathcal{N}(\mathbf{0}, \mathbf{W})$, where $\mathbf{W} \succ \mathbf{0}$. For the measurement noise in (1b), $\mathbf{v}_i(t) \sim \mathcal{N}(\mathbf{0}, \mathbf{V}_i)$, with $\mathbf{V}_i \succ \mathbf{0}$. Moreover, the processes $\mathbf{w}(t)$ and $\mathbf{v}_i(t)$, as well as $\mathbf{v}_i(t)$ and $\mathbf{v}_j(t)$ for $i \neq j$, are uncorrelated.

Remark 1: Note that our model (1) applies to a broad class of systems. This formulation subsumes (but is not limited to) the case of plants divided into N subsystems with dynamic couplings between them, where $\mathbf{x}(t)$ is a collection of the local subsystem states $\mathbf{x}_i(t)$, with local dynamics

$$\dot{\mathbf{x}}_i(t) = \textstyle\sum_{j=1}^{N} \mathbf{A}_{ij}\mathbf{x}_j(t) + \sum_{j=1}^{N} \mathbf{B}_{ij}\mathbf{u}_j(t) + \mathbf{w}_i(t),$$

where it is often assumed that $\mathbf{B}_{ij} = \mathbf{0}\ \forall j \neq i$, i.e. each actuator only directly affects its corresponding subsystem state, and the disturbances $\mathbf{w}_i(t)$ are uncorrelated, such as in [15]–[17], [22]. Our formulation is more general in this sense. In addition, we do not make any assumptions on the controllability and observability of local pairs of matrices.

The actuator nodes exchange information through a communication network, whose topology is described by an undirected and connected graph $\mathcal{G} = (\mathcal{V}, \mathcal{E})$. The node set is $\mathcal{V} = \{1, \dots, N\}$, representing the actuator nodes, while the edge set $\mathcal{E} \subseteq \mathcal{V} \times \mathcal{V}$ denotes the communication links between them. The adjacency matrix of $\mathcal{G}$ is denoted by $\mathbf{A}_{\mathcal{G}}$ and its Laplacian matrix by $\mathbf{L}_{\mathcal{G}}$. The set of communication neighbors for node i is given by $\mathcal{N}_i = \{j \in \mathcal{V} : (i,j) \in \mathcal{E}\}$.

We aim to collaboratively regulate system (1) in a distributed fashion, via output-feedback SMPC, where each actuator node computes its control input $\mathbf{u}_i(t)$ based on its measurement $\mathbf{y}_i(t)$ and local communication. Due to the partial and noisy measurements, a distributed state estimator is used so that each actuator node obtains local estimates $\hat{\mathbf{x}}_i(t)$ of the true state $\mathbf{x}(t)$. The nodes broadcast their local estimate only to their neighbors $j \in \mathcal{N}_i$. Furthermore, to save communication resources, information is transmitted only at sparse event instants. The sequence of communication events $\{\tau_\ell^i\}_{\ell=0}^{\infty}$ for node i is decided via a local event-triggering mechanism to be designed, based on node i's estimate.

Taking into account that the SMPC problem is solved by computing units in discrete-time and the potential computational cost of running the optimization, the computation of control inputs is solved periodically, at a series of discrete sampling instants $k \in \mathbb{Z}_{\geq 0}$. For this reason, we introduce the auxiliary sampled-data model for system (2), given by

$$\mathbf{x}(k+1) = \mathbf{A}_{\mathsf{d}}\mathbf{x}(k) + \mathbf{B}_{\mathsf{d}}\mathbf{u}(k) + \mathbf{w}_{\mathsf{d}}(k) \tag{3}$$

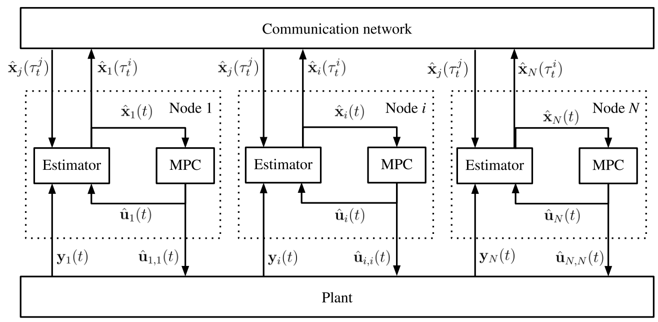

Fig. 1: Distributed SMPC setup.

for a sampling period h, where we use a forward Euler discretization with $\mathbf{A}_\mathsf{d} = \mathbf{I}_n + h\mathbf{A}$, $\mathbf{B}_\mathsf{d} = h\mathbf{B}$ and $\mathbf{w}_\mathsf{d}(k)$ is discrete-time white noise. For simplicity, we are using the notation $\mathbf{x}(k)$ to denote the state $\mathbf{x}(t)$ at $t = kh$. The system is subject to chance constraints on the states and hard constraints on the control inputs, to account for actuator saturation,

$$\mathbb{P}\{\mathbf{x}(k) \in \mathcal{X}\} \geq 1 - p_x, \quad \mathbf{u}(k) \in \mathcal{U}, \quad \forall k \geq 0, \tag{4}$$

where the input set $\mathcal{U} = \mathcal{U}_1 \times \cdots \times \mathcal{U}_N$, such that $\mathcal{U}_i$ represents the admissible set for the ith actuator. Moreover, $\mathcal{X}$ and $\mathcal{U}_i$, $i = 1, \ldots, N$, are bounded convex polytopes of appropriate dimensions containing the origin, and p_x is the allowable probability of violation for the state constraints for the system in closed loop with the controller.

The goal for our distributed SMPC controller is to find control inputs to collaboratively steer the state of system (3) to the origin under the constraints (4) in a receding horizon fashion. In addition, due to the presence of unbounded stochastic disturbances and hard input constraints, certain noise realizations might render the constrained optimization problem solved by the SMPC controller infeasible. For this reason, we also want to regulate the probability of losing feasibility of the optimization problem to be less than a user-defined threshold p_f.

III. Output-Feedback Distributed SMPC

To regulate the plant, each actuator node implements a distributed state estimator and MPC scheme, represented in Figure 1. The estimator at node i produces estimates $\hat{\mathbf{x}}_i(t) \in \mathbb{R}^{n_\mathbf{x}}$ for the state $\mathbf{x}(t)$, based on its measurement $\mathbf{y}_i(t)$ and communication with neighboring nodes. Then, an MPC scheme is solved at discrete instants $k \in \mathbb{Z}_{\geq 0}$ to compute the control inputs. Using its state estimate $\hat{\mathbf{x}}_i(k)$, each actuator node locally solves an optimization problem to compute an input $\hat{\mathbf{u}}_i(k)$. Note that $\hat{\mathbf{u}}_i(k) = [\hat{\mathbf{u}}_{i,1}(k)^\top, \ldots, \hat{\mathbf{u}}_{i,N}(k)^\top]^\top \in \mathbb{R}^{n_\mathbf{u}}$ is the ith node's belief about the actual input vector $\mathbf{u}(k) = [\mathbf{u}_1(k)^\top, \ldots, \mathbf{u}_N(k)^\top]^\top$, with $\hat{\mathbf{u}}_{i,j}(k)$ being its estimate of the input $\mathbf{u}_j(k)$ applied by the jth actuator node. Then, we set $\mathbf{u}_i(k) = \hat{\mathbf{u}}_{i,i}(k)$, which is applied in a sample-and-hold fashion to the system (1a), so that $\mathbf{u}_i(t) = \mathbf{u}_i(k)$ for $t \in [kh, (k+1)h)$. This means that each node i computes an input vector for the global system, but then applies only the elements corresponding to the ith actuator as its true input. The estimated inputs for the other actuator nodes are leveraged in the state estimator.

A. State Estimator

We adopt a similar approach as [23], where an estimator with event-triggered communication based on the asymptotic Kalman-Bucy filter is designed, for systems with no control inputs. In our case, we need to consider the addition of control inputs to the system. The input $\mathbf{u}(t)$ applied to the global system (2) is unknown from the point of view of each actuator node, as it depends on their local optimizations. For this reason, the input $\hat{\mathbf{u}}_i(t)$ computed locally by node i is used in the estimator as node i's estimate of $\mathbf{u}(t)$. Then, node i's estimate $\hat{\mathbf{x}}_i(t)$ of the state $\mathbf{x}(t)$ is given by

$$\begin{aligned}\dot{\hat{\mathbf{x}}}_i(t) &= \mathbf{A}\hat{\mathbf{x}}_i(t) + \mathbf{B}\hat{\mathbf{u}}_i(t) + \mathbf{K}_i\left(\mathbf{y}_i(t) - \mathbf{C}_i\hat{\mathbf{x}}_i(t)\right) \\ &\quad + \kappa\mathbf{P}_\infty \textstyle\sum_{j\in\mathcal{N}_i}(\hat{\mathbf{x}}_j(\tau_t^j) - \hat{\mathbf{x}}_i(t)),\end{aligned} \tag{5}$$

where $\mathbf{K}_i = N\mathbf{P}_\infty\mathbf{C}_i^\top\mathbf{V}_i^{-1}$, $\kappa > 0$ is the consensus gain, $\tau_t^j = \max\{\tau_\ell^j \leq t\}$ is the last communication event triggered by neighbor j prior to time t and $\mathbf{P}_\infty$ is the solution to

$$\mathbf{0} = \mathbf{A}\mathbf{P}_\infty + \mathbf{P}_\infty\mathbf{A}^\top + \mathbf{B}\mathbf{W}\mathbf{B}^\top - \mathbf{P}_\infty\mathbf{C}^\top\mathbf{V}^{-1}\mathbf{C}\mathbf{P}_\infty,$$

recalling $\mathbf{A}, \mathbf{B}, \mathbf{C}$ are the matrices from the global system (2) and $\mathbf{V} = \mathsf{diag}_{i=1}^N(\mathbf{V}_i)$ is the global measurement noise. The event-triggering mechanism is given by

$$\tau_{\ell+1}^i = \inf\{t > \tau_\ell^i + \underline{\tau} \;\mid\; \|\hat{\mathbf{x}}_i(t) - \hat{\mathbf{x}}_i(\tau_\ell^i)\| \geq \delta_i\}, \tag{6}$$

for some threshold $\delta_i \geq 0$. This triggering condition intuitively means that the current state estimate is only transmitted when it differs significantly from the last transmitted value, with the admissible difference being set by the parameter δ_i. If $\delta_i \to 0$, the full communication case is recovered. Due to the presence of Gaussian noise in the measurements, $\underline{\tau} > 0$ is introduced as time regularization to avoid the Zeno phenomenon [24]. In practice, $\underline{\tau}$ can be set arbitrarily small so that its effect is negligible. In order to guarantee the stability of the estimation error from (5), we consider the following for simplicity:

Assumption 3: The gain κ in (5) is set such that $\mathbf{A}_{\tilde{\mathbf{x}}} = \mathsf{diag}_{i=1}^N\left(\mathbf{A} - \mathbf{K}_i\mathbf{C}_i\right) - \kappa\left(\mathbf{L}_\mathcal{G} \otimes \mathbf{P}_\infty\right)$ is Hurwitz stable.

According to [23, Proposition 1], there exists a gain $\kappa_0 > 0$ such that, for any $\kappa > \kappa_0$, Assumption 3 is fulfilled; moreover, a suitable κ, as well as $\mathbf{P}_\infty$, can be computed in a distributed fashion as shown in [25].

B. MPC Controller

We adopt a tube-based approach to design the MPC controller, similarly to other works featuring stochastic and robust MPC, e.g. [4]–[6], [22], [26]. At each discrete step $k \in \mathbb{Z}_{\geq 0}$ where the MPC problem is solved, we divide the m-steps ahead estimate $\hat{\mathbf{x}}_i(m|k)$, relative to step k, into

$$\hat{\mathbf{x}}_i(m|k) = \mathbf{z}_i(m|k) + \mathbf{e}_i(m|k),$$

where $\mathbf{z}_i(m|k)$ represents the nominal (undisturbed) trajectory of the system, predicted by node i, and $\mathbf{e}_i(m|k)$ is related to the disturbances. Similarly, we parameterize the predicted control inputs computed by the optimization problem at the ith actuator node as

$$\hat{\mathbf{u}}_i(m|k) = \mathbf{c}_i(m|k) + \mathbf{L}\mathbf{e}_i(m|k), \tag{7}$$

where $\mathbf{c}_i(m|k)$ is the m-steps ahead nominal input computed by the optimization at the ith node at step k. The control gain $\mathbf{L}$ is chosen such that the closed-loop matrix $\mathbf{A}_{\mathsf{cl}} = \mathbf{A}_{\mathsf{d}} + \mathbf{B}_{\mathsf{d}}\mathbf{L}$ is Schur stable. Considering the nominal inputs $\mathbf{c}_i(m|k)$ computed by node i, its prediction for the nominal trajectory of the system is

$$\mathbf{z}_i(m+1|k) = \mathbf{A}_{\mathsf{d}}\mathbf{z}_i(m|k) + \mathbf{B}_{\mathsf{d}}\mathbf{c}_i(m|k). \tag{8}$$

The nominal dynamics (8) allow to reformulate the stochastic problem into a deterministic one, by solving an optimal control problem on the nominal predicted states and inputs, while the additional term $\mathbf{L}\mathbf{e}_i(m|k)$ in (7) aims to keep the error around the nominal trajectory close to zero with a pre-stabilizing gain. Then, the MPC controller at the ith node solves the following constrained optimization problem at each time step k:

$$\min_{\mathbb{Z}_i,\mathbb{C}_i} \sum_{m=0}^{T-1} \left(\|\mathbf{z}_i(m|k)\|^2_{\mathbf{Q}} + \|\mathbf{c}_i(m|k)\|^2_{\mathbf{R}}\right) + \|\mathbf{z}_i(T|k)\|^2_{\mathbf{Q}_f} \tag{9a}$$

$$\text{s.t. } \mathbf{z}_i(m+1|k) = \mathbf{A}_{\mathsf{d}}\mathbf{z}_i(m|k) + \mathbf{B}_{\mathsf{d}}\mathbf{c}_i(m|k), \quad m = 0,\dots,T-1, \tag{9b}$$

$$\mathbf{z}_i(0|k) = \hat{\mathbf{x}}_i(k), \tag{9c}$$

$$\mathbf{z}_i(m|k) \in \mathcal{Z}_{i,m},\ \mathbf{c}_i(m|k) \in \mathcal{C}_{i,m}, m = 0,\dots,T-1, \tag{9d}$$

$$\mathbf{z}_i(T|k) \in \mathcal{Z}_{i,f}. \tag{9e}$$

Here, $T \in \mathbb{Z}_{>0}$ is the finite optimization horizon (we consider the same length for the prediction and control horizons), and $\mathbf{Q} \succ \mathbf{0}$, $\mathbf{R} \succ \mathbf{0}$ are appropriate weighting matrices, with $\mathbf{Q}_f \succ \mathbf{0}$ being the weighting matrix for the terminal cost. $\mathbb{Z}_i = \{\mathbf{z}_i(0|k),\dots,\mathbf{z}_i(T|k)\}$ and $\mathbb{C}_i = \{\mathbf{c}_i(0|k),\dots,\mathbf{c}_i(T-1|k)\}$ are the predicted sequences of nominal states and inputs to be optimized, respectively. The constraint (9b) constitutes the predicted evolution of the nominal system according to the information available to node i, while (9c) provides the initialization of the nominal predicted states, taking into account the available state estimate at node i. $\mathcal{Z}_{i,m}$ and $\mathcal{C}_{i,m}$ in (9d) represent the m-step ahead tightened constraints for the nominal states and inputs at node i, with $\mathcal{Z}_{i,f}$ in (9e) being a terminal set. The design of these sets will be addressed in Section IV, so that the original constraints (4) on the system with stochastic noise can be fulfilled while each actuator node solves (9) on its nominal prediction. At each time step k, each node solves (9) to compute a sequence of nominal inputs $\mathbb{C}_i$. Considering (7), $\hat{\mathbf{u}}_i(k) = \mathbf{c}_i(0|k)$, since $\mathbf{e}_i(0|k) = \hat{\mathbf{x}}_i(k) - \mathbf{z}_i(0|k) = \mathbf{0}$. Then, node i applies elements corresponding to the ith actuator as its real input, i.e. $\mathbf{u}_i(k) = \hat{\mathbf{u}}_{i,i}(k)$.

Assumption 4: The estimator (5) and the MPC controller (9) are initialized at $t = 0$, $k = 0$ to the initial state $\mathbf{z}_i(0|0) = \hat{\mathbf{x}}_i(0) = \mathbf{x}_0,\ \forall i \in \mathcal{V}$, for which the optimization problem (9) is feasible, i.e. there exists a sequence of inputs for which the constraints (9b)-(9e) are satisfied.

Remark 2: Computing suitable constraints $\mathcal{Z}_{i,m}$, $\mathcal{Z}_{i,f}$, $\mathcal{C}_{i,m}$ for the optimization problem (9) requires the consideration of the interactions and information flow in the network of actuator nodes, for which a global view of the coupled behavior of the system is needed. For this reason, and to avoid using communication-intensive approaches such as distributed optimization, our constraint design is performed offline. We consider that the designer has full information about the plant and measurement models of all N actuator nodes, knowing $\mathbf{A}, \mathbf{B}, \mathbf{W}, \mathbf{C}_i, \mathbf{V}_i, \forall i \in \mathcal{V}$, the event thresholds δ_i, the matrices $\mathbf{A}_{\mathcal{G}}, \mathbf{L}_{\mathcal{G}}$ for the communication graph, the constraint data $\mathcal{X}, \mathcal{U}, p_x$, and the choice of MPC parameters $T, \mathbf{Q}, \mathbf{R}, \mathbf{Q}_f, p_f$. During online execution, each node implements (5), (6) and (9), for which it requires knowledge of the plant matrices $\mathbf{A}, \mathbf{B}$, its local measurement model $\mathbf{C}_i, \mathbf{V}_i$ and event threshold δ_i, the predefined gains κ, $\mathbf{K}_i$, $\mathbf{P}_\infty$, the MPC parameters, and the tightened constraints $\mathcal{Z}_{i,m}, \mathcal{C}_{i,m}, m = 0,\dots,T-1$ and $\mathcal{Z}_{i,f}$. These are all constant parameters set during the offline design phase. Online, each node takes local measurements $\mathbf{y}_i(t)$ and receives state estimates $\hat{\mathbf{x}}_j(\tau_k^j)$ from its neighbors $j \in \mathcal{N}_i$ only at event instants, which it uses to compute its local state estimates $\hat{\mathbf{x}}_i(t)$ and control inputs $\mathbf{u}_i(t)$. Therefore, the online execution remains distributed in this sense.

IV. Constraint Design

In this section, we adapt the sets $\mathcal{X}, \mathcal{U}$ from the original constraints (4) into appropriate sets $\mathcal{Z}_{i,m}, \mathcal{C}_{i,m}$ to be used in the optimization problem (9), such that imposing the constraints (9d) on the predicted nominal states $\mathbf{z}_i(m|k)$ and inputs $\mathbf{c}_i(m|k)$ at each node results in the satisfaction of (4) for $\mathbf{x}(k)$, $\mathbf{u}(k)$ of the global system subject to stochastic noise and the desired regulation of the loss of feasibility for the optimization problem. There are two sources of error between the true state and the nominal one (8). Namely, the estimation error $\tilde{\mathbf{x}}_i(k) = \mathbf{x}(k) - \hat{\mathbf{x}}_i(k)$ between the real state and the estimate used in (9c) to initialize the optimization problem, and the predicted control error $\mathbf{e}_i(m|k) = \hat{\mathbf{x}}_i(m|k) - \mathbf{z}_i(m|k)$ due to the difference between the actual estimate available at step $k+m$ and the predicted nominal trajectory. Considering both errors, the m-steps ahead state can be divided into

$$\mathbf{x}(m|k) = \mathbf{z}_i(m|k) + \tilde{\mathbf{x}}_i(m|k) + \mathbf{e}_i(m|k), \tag{10}$$

while the predicted input $\hat{\mathbf{u}}_i(m|k)$ is divided into a nominal part $\mathbf{c}_i(m|k)$ and a correction of the control error $\mathbf{L}\mathbf{e}_i(m|k)$, recalling (7). Thus, the constraints need to be adapted by taking into account these two errors. We take a similar approach as in [6], where uniformly bounded confidence sets are designed for the errors and then used for constraint tightening. We first recall the definition and design of such sets:

Definition 1 (Adapted from [6]): A set $\mathcal{S}_p^{\mathbf{r}}$ is a uniformly bounded confidence set of probability p for a random variable $\mathbf{r}(t)$ if $\mathbb{P}(\mathbf{r}(t) \in \mathcal{S}_p^{\mathbf{r}}) \geq p,\ \forall t \geq 0$.

Lemma 1 (Adapted from [6], Lemma 1): Consider $\mathbf{r}(t) \in \mathbb{R}^{n_{\mathbf{r}}} \sim \mathcal{N}(\mathbf{0}, \mathbf{\Sigma}(t))$, with $\mathbf{\Sigma}$ being a uniform upper bound of $\mathbf{\Sigma}(t)$, such that $\mathbf{\Sigma}(t) \preceq \mathbf{\Sigma},\ \forall t \geq 0$. Let $\mathcal{S}_{1-p}^{\mathbf{r}} = \{\mathbf{r}(t) : \mathbf{H}_r\mathbf{r}(t) \leq \mathbf{h}_r,\ \forall t \geq 0\}$, where $[\mathbf{h}_r]_m = \mathit{cdf}^{-1}(1-p_m)\sqrt{[\mathbf{H}_r]_m \mathbf{\Sigma} [\mathbf{H}_r]_m^\top}$, $\sum_{m=1}^{n_{\mathbf{r}}} p_m = p$, with $p_m \in (0,1)$ for $m = 1,\dots,n_{\mathbf{r}}$, where $\mathbf{H}_r$ is a design parameter and $\mathit{cdf}^{-1}(\bullet)$ denotes the inverse of the cumulative Gaussian distribution function. Then, $\mathcal{S}_{1-p}^{\mathbf{r}}$ is a uniformly bounded confidence set of probability $1-p$ for the variable $\mathbf{r}(t)$.

Proof: The proof follows by the same arguments as [6, Lemma 1], which was originally given for a discrete-time variable $\mathbf{r}(k)$. ■

By analyzing the error dynamics, we design such sets where the disturbances are contained with no less than the desired probability. Then, we use them to tighten $\mathcal{X}, \mathcal{U}$ into $\mathcal{Z}_{i,m}, \mathcal{C}_{i,m}$. Note that, due to our distributed setup where each actuator node has partial information and exchanges data with neighboring nodes to jointly achieve the control task, providing an approach to extend the centralized proposal from [6] to our distributed case is not trivial, as it requires analysis of the coupled error dynamics between nodes.

A. State Estimation Error Dynamics

Considering the local measurement (1b), the system dynamics (2), the estimator (5) and event-triggering condition (6), we can write the error dynamics of the estimate in node i as

$$\begin{aligned}
\dot{\tilde{\mathbf{x}}}_i(t) &= \dot{\mathbf{x}}(t) - \dot{\hat{\mathbf{x}}}_i(t) \\
&= \mathbf{A}\mathbf{x}(t) + \mathbf{B}\mathbf{u}(t) + \mathbf{w}(t) - \mathbf{A}\hat{\mathbf{x}}_i(t) - \mathbf{B}\hat{\mathbf{u}}_i(t) \\
&\quad - \mathbf{K}_i\mathbf{C}_i\mathbf{x}(t) - \mathbf{K}_i\mathbf{v}_i(t) + \mathbf{K}_i\mathbf{C}_i\hat{\mathbf{x}}_i(t) \\
&\quad - \kappa\mathbf{P}_\infty \textstyle\sum_{j\in\mathcal{N}_i} (\hat{\mathbf{x}}_j(t) - \hat{\mathbf{x}}_i(t)) + \kappa\mathbf{P}_\infty \sum_{j\in\mathcal{N}_i} \mathbf{n}_j(t) \\
&= (\mathbf{A} - \mathbf{K}_i\mathbf{C}_i)\,\tilde{\mathbf{x}}_i(t) + \mathbf{B}(\mathbf{u}(t) - \hat{\mathbf{u}}_i(t)) + \mathbf{w}(t) - \mathbf{K}_i\mathbf{v}_i(t) \\
&\quad - \kappa\mathbf{P}_\infty \textstyle\sum_{j\in\mathcal{N}_i} (\tilde{\mathbf{x}}_i(t) - \tilde{\mathbf{x}}_j(t)) + \kappa\mathbf{P}_\infty \sum_{j\in\mathcal{N}_i} \mathbf{n}_j(t),
\end{aligned} \tag{11}$$

where we have defined $\mathbf{n}_j(t) = \hat{\mathbf{x}}_j(t) - \hat{\mathbf{x}}_j(\tau_t^i)$ as the event-triggered error between the current estimate $\hat{\mathbf{x}}_j(t)$ from neighbor j and its latest transmitted value $\hat{\mathbf{x}}_j(\tau_t^j)$. Letting $\tilde{\mathbf{x}}(t) = \mathsf{col}_{i=1}^N(\tilde{\mathbf{x}}_i(t))$, $\hat{\mathbf{u}}(t) = \mathsf{col}_{i=1}^N(\hat{\mathbf{u}}_i(t))$ and $\mathbf{n}(t) = \mathsf{col}_{i=1}^N(\mathbf{n}_i(t))$, the aggregate dynamics are

$$\begin{aligned}
\dot{\tilde{\mathbf{x}}}(t) &= (\mathsf{diag}_{i=1}^N (\mathbf{A} - \mathbf{K}_i\mathbf{C}_i) - \kappa\,(\mathbf{L}_\mathcal{G} \otimes \mathbf{P}_\infty))\tilde{\mathbf{x}}(t) \\
&\quad + (\mathbf{I}_N \otimes \mathbf{B})(\mathbb{1}_N \otimes \mathbf{u}(t) - \hat{\mathbf{u}}(t)) + \kappa(\mathbf{A}_\mathcal{G} \otimes \mathbf{P}_\infty)\mathbf{n}(t) \\
&\quad + \mathbb{1}_N \otimes \mathbf{w}(t) - \mathsf{diag}_{i=1}^N(\mathbf{K}_i)\mathbf{v}(t) \\
&= \mathbf{A}_{\tilde{\mathbf{x}}}\tilde{\mathbf{x}}(t) + (\mathbf{I}_N \otimes \mathbf{B})\tilde{\mathbf{u}}(t) + \kappa(\mathbf{A}_\mathcal{G} \otimes \mathbf{P}_\infty)\mathbf{n}(t) \\
&\quad + \mathbb{1}_N \otimes \mathbf{w}(t) - \mathbf{K}\mathbf{v}(t),
\end{aligned}$$

where we have defined the control mismatch $\tilde{\mathbf{u}}(t) = \mathbb{1}_N \otimes \mathbf{u}(t) - \hat{\mathbf{u}}(t)$, $\mathbf{K} = \mathsf{diag}_{i=1}^N(\mathbf{K}_i)$, and we have used the matrix $\mathbf{A}_{\tilde{\mathbf{x}}}$ defined in Assumption 3. The dynamics of $\tilde{\mathbf{x}}(t)$ contain both stochastic terms due to the presence of Gaussian noises, and other bounded terms due to the input mismatch $\tilde{\mathbf{u}}(t)$ and the event-triggered error $\mathbf{n}(t)$. In contrast, the design of confidence sets is given in Lemma 1 for a normally distributed random variable with zero mean and known covariance. Hence, we separate $\tilde{\mathbf{x}}(t)$ into a deterministic part $\tilde{\mathbf{x}}^d(t)$, for which we will find a bounded set that contains the disturbance $\forall t$, and a stochastic part $\tilde{\mathbf{x}}^s(t)$ for which we will construct a set as in Lemma 1. Letting $\tilde{\mathbf{x}}(t) = \tilde{\mathbf{x}}^d(t) + \tilde{\mathbf{x}}^s(t)$, we have

$$\dot{\tilde{\mathbf{x}}}^d(t) = \mathbf{A}_{\tilde{\mathbf{x}}}\tilde{\mathbf{x}}^d(t) + (\mathbf{I}_N \otimes \mathbf{B})\tilde{\mathbf{u}}(t) + \kappa(\mathbf{A}_\mathcal{G} \otimes \mathbf{P}_\infty)\mathbf{n}(t), \tag{12a}$$

$$\dot{\tilde{\mathbf{x}}}^s(t) = \mathbf{A}_{\tilde{\mathbf{x}}}\tilde{\mathbf{x}}^s(t) + \mathbb{1}_N \otimes \mathbf{w}(t) - \mathbf{K}\mathbf{v}(t). \tag{12b}$$

With $\hat{\mathbf{x}}_i(0) = \mathbf{x}_0$ from Assumption 4, we have $\tilde{\mathbf{x}}^d(0) = \mathbf{0}$, $\mathbb{E}\{\tilde{\mathbf{x}}^s(0)\} = \mathbf{0}$. Then, $\tilde{\mathbf{x}}^s(t) \sim \mathcal{N}(\mathbf{0}, \mathbf{X}^s(t))$, with zero mean due to $\mathbb{E}\{\mathbf{w}(t)\} = \mathbf{0}$ and $\mathbb{E}\{\mathbf{v}(t)\} = \mathbf{0}$, $\forall t$, and the covariance $\mathbf{X}^s(t)$ is given by $\mathbf{X}^s(0) = \mathbf{I}_N \otimes \mathbf{P}_0$ and

$$\dot{\mathbf{X}}^s(t) = \mathbf{A}_{\tilde{\mathbf{x}}}\mathbf{X}^s(t) + \mathbf{X}^s(t)\mathbf{A}_{\tilde{\mathbf{x}}}^\top + \mathbb{1}\mathbb{1}^\top \otimes \mathbf{W} + \mathbf{K}\mathbf{V}\mathbf{K}^\top. \tag{13}$$

B. Predictive Control Error Dynamics

Now, we tackle the error $\mathbf{e}_i(m|k)$ in (7)-(10). Since the MPC is solved in discrete time, consider the following discretized dynamics for the m-steps ahead state estimates, which we obtain using the Euler discretization of (5), to aid in computing the control error dynamics:

$$\begin{aligned}
&\hat{\mathbf{x}}_i(m+1|k) = \mathbf{A}_\mathsf{d}\hat{\mathbf{x}}_i(m|k) + \mathbf{B}_\mathsf{d}\hat{\mathbf{u}}_i(m|k) \\
&\quad + h\mathbf{K}_i\,(\mathbf{y}_i(m|k) - \mathbf{C}_i\hat{\mathbf{x}}_i(m|k)) - h\kappa\mathbf{P}_\infty \textstyle\sum_{j\in\mathcal{N}_i} \mathbf{n}_j(m|k) \\
&\quad + h\kappa\mathbf{P}_\infty \textstyle\sum_{j\in\mathcal{N}_i} (\hat{\mathbf{x}}_j(m|k) - \hat{\mathbf{x}}_i(m|k)).
\end{aligned} \tag{14}$$

Then, considering the nominal predicted dynamics (8) and the predicted inputs (7), we have

$$\begin{aligned}
&\mathbf{e}_i(m+1|k) = \hat{\mathbf{x}}_i(m+1|k) - \mathbf{z}_i(m+1|k) \\
&= (\mathbf{A}_\mathsf{d} + \mathbf{B}_\mathsf{d}\mathbf{L})\mathbf{e}_i(m|k) + h\mathbf{K}_i\mathbf{C}_i\tilde{\mathbf{x}}_i(m|k) + h\mathbf{K}_i\mathbf{v}_i(m|k) \\
&\quad + h\kappa\mathbf{P}_\infty \sum_{j\in\mathcal{N}_i} (\tilde{\mathbf{x}}_i(m|k) - \tilde{\mathbf{x}}_j(m|k)) - h\kappa\mathbf{P}_\infty \sum_{j\in\mathcal{N}_i} \mathbf{n}_j(m|k) \\
&= \mathbf{A}_\mathsf{cl}\mathbf{e}_i(m|k) + \mathbf{d}_i(m|k) \\
&= \textstyle\sum_{q=0}^m \mathbf{A}_\mathsf{cl}^{m-q}\mathbf{d}_i(q|k),
\end{aligned} \tag{15}$$

where the last line results from $\mathbf{e}_i(0|k) = \hat{\mathbf{x}}_i(k) - \mathbf{z}_i(0|k) = \mathbf{0}$ due to (9c). Thus, we are interested in finding a set containing the disturbance

$$\begin{aligned}
&\mathbf{d}_i(m|k) = h\mathbf{K}_i\mathbf{C}_i\tilde{\mathbf{x}}_i(m|k) + h\mathbf{K}_i\mathbf{v}_i(m|k) \\
&\quad + h\kappa\mathbf{P}_\infty \sum_{j\in\mathcal{N}_i} (\tilde{\mathbf{x}}_i(m|k) - \tilde{\mathbf{x}}_j(m|k)) - h\kappa\mathbf{P}_\infty \sum_{j\in\mathcal{N}_i} \mathbf{n}_j(m|k),
\end{aligned}$$

noting that it involves terms related to neighbor information. Stacking the dynamics for all nodes as $\mathbf{e}(m|k) = \mathsf{col}_{i=1}^N(\mathbf{e}_i(m|k))$, we have

$$\begin{aligned}
\mathbf{e}(m+1|k) &= (\mathbf{I}_n \otimes \mathbf{A}_\mathsf{cl})\mathbf{e}(m|k) + h\mathbf{K}\mathbf{v}(m|k) \\
&\quad + h(\mathsf{diag}_{i=1}^N(\mathbf{K}_i\mathbf{C}_i) + \kappa(\mathbf{L}_\mathcal{G} \otimes \mathbf{P}_\infty))\tilde{\mathbf{x}}(m|k) \\
&\quad - h\kappa(\mathbf{A}_\mathcal{G} \otimes \mathbf{P}_\infty)\mathbf{n}(m|k) \\
&= \mathbf{A}_\mathbf{e}\mathbf{e}(m|k) + h\mathbf{B}_\mathbf{e}\tilde{\mathbf{x}}^d(m|k) + h\mathbf{B}_\mathbf{e}\tilde{\mathbf{x}}^s(m|k) \\
&\quad - h\kappa(\mathbf{A}_\mathcal{G} \otimes \mathbf{P}_\infty)\mathbf{n}(m|k) + h\mathbf{K}\mathbf{v}(m|k) \\
&= \mathbf{A}_\mathbf{e}\mathbf{e}(m|k) + \mathbf{d}(m|k),
\end{aligned} \tag{16}$$

where we have defined $\mathbf{A}_\mathbf{e} = \mathbf{I}_N \otimes \mathbf{A}_\mathsf{cl}$, $\mathbf{B}_\mathbf{e} = \mathsf{diag}_{i=1}^N(\mathbf{K}_i\mathbf{C}_i) + \kappa(\mathbf{L}_\mathcal{G} \otimes \mathbf{P}_\infty)$, and in the second equality we have split $\tilde{\mathbf{x}}(m|k)$ into a stochastic part $\tilde{\mathbf{x}}^s(m|k)$ and a deterministic part $\tilde{\mathbf{x}}^d(m|k)$, recalling (12a)-(12b). Similarly, we split $\mathbf{d}(m|k)$ in (16) into $\mathbf{d}(m|k) = \mathbf{d}^d(m|k) + \mathbf{d}^s(m|k)$, with

$$\mathbf{d}^d(m|k) = h\mathbf{B}_\mathbf{e}\tilde{\mathbf{x}}^d(m|k) - h\kappa(\mathbf{A}_\mathcal{G} \otimes \mathbf{P}_\infty)\mathbf{n}(m|k), \tag{17a}$$

$$\mathbf{d}^s(m|k) = h\mathbf{B}_\mathbf{e}\tilde{\mathbf{x}}^s(m|k) + h\mathbf{K}\mathbf{v}(m|k). \tag{17b}$$

Noting that $\mathbb{E}\{\tilde{\mathbf{x}}^s(m|k)\} = \mathbf{0}$ and $\mathbb{E}\{\mathbf{v}(m|k)\} = \mathbf{0}$, $\mathbf{d}^s(m|k) \sim \mathcal{N}(\mathbf{0}, \mathbf{D}^s(m|k))$ with its covariance given by

$$\mathbf{D}^s(m|k) = h^2\mathbf{B}_\mathbf{e}\mathbf{X}^s(m|k)\mathbf{B}_\mathbf{e}^\top + h^2\mathbf{K}\mathbf{V}\mathbf{K}^\top, \tag{18}$$

where $\mathbf{X}^s(m|k) = \mathsf{cov}\{\tilde{\mathbf{x}}^s(m|k)\}$, recalling the covariance's dynamics (13). With this information, we can design a bounded set that contains the deterministic disturbance $\mathbf{d}_i^d(m|k)$ $\forall m, k$ and a uniformly bounded confidence set for the stochastic disturbance $\mathbf{d}_i^s(m|k)$.

C. Sets for Deterministic Disturbances

First, we address the deterministic disturbance terms, which evolve according to the aggregate dynamics (12a) and (17a). Note that they contain the effect of the control mismatch $\tilde{\mathbf{u}}(t)$ and the event-triggered error $\mathbf{n}(t)$. Since the set $\mathcal{U}$ is a bounded polytope, we can find an outer approximation $\mathcal{U}' = \{\mathbf{u}' \in \mathbb{R}^{n_\mathbf{u}} : \underline{\mathbf{u}} \leq \mathbf{u}' \leq \bar{\mathbf{u}}\}$ for some lower and upper bounds $\underline{\mathbf{u}}$, $\bar{\mathbf{u}} \in \mathbb{R}^{n_\mathbf{u}}$, such that $\mathcal{U} \subseteq \mathcal{U}'$. Then, we have for the control mismatch $\tilde{\mathbf{u}}(t)$ that

$$\|\tilde{\mathbf{u}}(t)\| = \|\mathbb{1}_N \otimes \mathbf{u}(t) - \hat{\mathbf{u}}(t)\| \leq \sqrt{N-1}\|\bar{\mathbf{u}} - \underline{\mathbf{u}}\| =: U,\ \forall t, \tag{19}$$

noting that each actuator node estimates its own input exactly due to $\mathbf{u}_i(k) = \hat{\mathbf{u}}_{i,i}(k)$. In addition, the event-triggered error fulfills $\|\mathbf{n}(t)\| \leq \sqrt{N}\delta_{\max}$ due to the design of the event-triggering condition (6), with $\delta_{\max} = \max\{\delta_i\}_{i=1}^N$ being the maximum event threshold. Then, the following Lemma summarizes the design of bounded sets for the deterministic disturbances at each node.

Lemma 2: Let Assumptions 1 to 4 hold. Define $\mathcal{S}^{\tilde{\mathbf{x}}_i^d} = \{\mathbf{x} \in \mathbb{R}^{n_\mathbf{x}} : \|\mathbf{x}\| \leq X^d\}$ and $\mathcal{S}^{\mathbf{d}_i^d} = \{\mathbf{x} \in \mathbb{R}^{n_\mathbf{x}} : \|\mathbf{x}\| \leq D^d\}$ with

$$\begin{aligned} X^d &= (\|\mathbf{B}\|U + \kappa\|\mathbf{A}_\mathcal{G} \otimes \mathbf{P}_\infty\|\sqrt{N}\delta_{\max})/|\lambda_{\max}(\mathbf{A}_{\tilde{\mathbf{x}}})|, \\ D^d &= h\|\mathbf{B_e}\|X^d + h\kappa\|\mathbf{A}_\mathcal{G} \otimes \mathbf{P}_\infty\|\sqrt{N}\delta_{\max}. \end{aligned} \tag{20}$$

Consider the variables $\tilde{\mathbf{x}}_i^d(t)$ and $\mathbf{d}_i^d(m|k)$, given for all nodes $i \in \mathcal{V}$ by the dynamics (12a) and (17a), respectively. Then, $\tilde{\mathbf{x}}_i^d(t) \in \mathcal{S}^{\tilde{\mathbf{x}}_i^d}$ $\forall t$, and $\mathbf{d}_i^d(m|k) \in \mathcal{S}^{\mathbf{d}_i^d}$ $\forall m, k$.

Proof: For the aggregate variable $\tilde{\mathbf{x}}^d(t)$, the dynamics (12a) have the following explicit solution,

$$\begin{aligned} \tilde{\mathbf{x}}^d(t) = e^{\mathbf{A}_{\tilde{\mathbf{x}}}t}\tilde{\mathbf{x}}^d(0) &+ \textstyle\int_0^t \exp(\mathbf{A}_{\tilde{\mathbf{x}}}\tau)(\mathbf{I}_N \otimes \mathbf{B})\tilde{\mathbf{u}}(t-\tau)\mathrm{d}\tau \\ &- \textstyle\int_0^t \kappa \exp(\mathbf{A}_{\tilde{\mathbf{x}}}\tau)(\mathbf{A}_\mathcal{G} \otimes \mathbf{P}_\infty)\mathbf{n}(t-\tau)\mathrm{d}\tau. \end{aligned}$$

The first term equals zero with the initialization $\hat{\mathbf{x}}_i(0) = \mathbf{x}_0$ from Assumption 4. For the rest, we compute a uniform bound for $\|\tilde{\mathbf{x}}^d(t)\|$ as follows,

$$\begin{aligned} \|\tilde{\mathbf{x}}^d(t)\| &\leq \|\mathbf{B}\| \sup_{s\geq 0}(\|\tilde{\mathbf{u}}(s)\|) \textstyle\int_0^t \|\exp(\mathbf{A}_{\tilde{\mathbf{x}}}\tau)\|\mathrm{d}\tau \\ &+ \kappa\|\mathbf{A}_\mathcal{G} \otimes \mathbf{P}_\infty\| \sup_{s\geq 0}(\|\mathbf{n}(s)\|) \textstyle\int_0^t \|\exp(\mathbf{A}_{\tilde{\mathbf{x}}}\tau)\|\mathrm{d}\tau \\ &\leq \|\mathbf{B}\|U \textstyle\int_0^t \exp(\lambda_{\max}(\mathbf{A}_{\tilde{\mathbf{x}}})\tau)\mathrm{d}\tau \\ &+ \kappa\|\mathbf{A}_\mathcal{G} \otimes \mathbf{P}_\infty\|\sqrt{N}\delta_{\max} \textstyle\int_0^t \exp(\lambda_{\max}(\mathbf{A}_{\tilde{\mathbf{x}}})\tau)\mathrm{d}\tau \\ &= \frac{\|\mathbf{B}\|U + \kappa\|\mathbf{A}_\mathcal{G} \otimes \mathbf{P}_\infty\|\sqrt{N}\delta_{\max}}{\lambda_{\max}(\mathbf{A}_{\tilde{\mathbf{x}}})}(\exp(\lambda_{\max}(\mathbf{A}_{\tilde{\mathbf{x}}})t) - 1) \\ &\leq \frac{\|\mathbf{B}\|U + \kappa\|\mathbf{A}_\mathcal{G} \otimes \mathbf{P}_\infty\|\sqrt{N}\delta_{\max}}{|\lambda_{\max}(\mathbf{A}_{\tilde{\mathbf{x}}})|} =: X^d,\ \forall t \geq 0, \end{aligned}$$

where we have used that $\|\exp(\mathbf{A}_{\tilde{\mathbf{x}}}t)\| \leq \exp(\lambda_{\max}(\mathbf{A}_{\tilde{\mathbf{x}}})t)$ and $\lambda_{\max}(\mathbf{A}_{\tilde{\mathbf{x}}}) < 0$, since $\mathbf{A}_{\tilde{\mathbf{x}}}$ is Hurwitz due to Assumption 3. Evidently, $\|\tilde{\mathbf{x}}^d(t)\| \leq X^d$ implies $\|\tilde{\mathbf{x}}_i^d(t)\| \leq X^d$ for each node by using the triangle inequality, from which the design of the set $\mathcal{S}^{\tilde{\mathbf{x}}_i^d}$ containing $\tilde{\mathbf{x}}_i(t)$ follows. Similarly, for the control disturbance $\mathbf{d}^d(m|k)$ given by (17a), we can compute a bound as

$$\|\mathbf{d}^d(m|k)\| \leq h\|\mathbf{B_e}\|X^d + h\kappa\|\mathbf{A}_\mathcal{G} \otimes \mathbf{P}_\infty\|\sqrt{N}\delta_{\max} =: D^d,$$

from which we design the appropriate set $\mathcal{S}^{\mathbf{d}_i^d}$. ■

D. Confidence Sets for Stochastic Disturbances

Now, we construct sets $\mathcal{S}_{1-p_x}^{\tilde{\mathbf{x}}_i^s}$ and $\mathcal{S}_{1-p_f}^{\mathbf{d}_i^s}$ for the random variables $\tilde{\mathbf{x}}_i^s(t)$ and $\mathbf{d}_i^s(m|k)$, recalling that p_x is the admissible violation of state constraints in (4), and the probability p_f regulates the loss of feasibility. To construct the sets according to Lemma 1, we first need to find uniform upper bounds on their covariances.

The covariance for $\tilde{\mathbf{x}}^s(t)$ is given by (13). Recall that the consensus gain κ in (5) is chosen such that $\mathbf{A}_{\tilde{\mathbf{x}}}$ is Hurwitz, meaning that $\tilde{\mathbf{x}}^s(t)$ has stable dynamics. Therefore, from the stable dynamics and the covariance matrices $\mathbf{W}, \mathbf{V}$ being constant, it follows that a uniform upper bound exists for $\mathbf{X}^s(t)$. Moreover, since the sum $\mathbb{1}\mathbb{1}^\top \otimes \mathbf{W} + \mathbf{KVK}^\top$ yields a positive definite matrix, (13) is a differential Lyapunov equation, which has a known explicit solution that reaches an equilibrium value $\mathbf{X}_\infty^s$ given by

$$\mathbf{0} = \mathbf{A}_{\tilde{\mathbf{x}}}\mathbf{X}_\infty^s + \mathbf{X}_\infty^s\mathbf{A}_{\tilde{\mathbf{x}}}^\top + \mathbb{1}\mathbb{1}^\top \otimes \mathbf{W} + \mathbf{KVK}^\top.$$

For ease of presentation, we will assume here that $\mathbf{X}_\infty^s$ is an upper bound fulfilling $\mathbf{X}^s(t) \preceq \mathbf{X}_\infty^s,\ \forall t \geq 0$, in analogy to [6] where the steady-state error covariance matrix for the centralized estimates is used. Nevertheless, an upper bound can also be found by evaluating the known explicit solution to (13). For the variable $\mathbf{d}^s(m|k)$, the covariance is given in (18). Then, $\mathbf{D}^s(m|k) \preceq h^2\mathbf{B_e}\mathbf{X}_\infty^s\mathbf{B_e}^\top + h^2\mathbf{KVK}^\top =: \mathbf{D}_\infty^s$.

Note that the matrices $\mathbf{X}_\infty^s, \mathbf{D}_\infty^s$ are dense due to the correlated estimation and prediction errors in the nodes. However, we want to find a uniform covariance upper bound for the disturbances $\tilde{\mathbf{x}}_i(t), \mathbf{d}_i(m|k)$ at each node, regardless of neighbor dynamics. To address this challenge, we adopt a similar strategy to [16], [22], [27] and introduce auxiliary positive semidefinite block-diagonal matrices $\bar{\mathbf{X}}^s = \mathsf{diag}_{i=1}^N(\bar{\mathbf{X}}_i^s)$ and $\bar{\mathbf{D}}^s = \mathsf{diag}_{i=1}^N(\bar{\mathbf{D}}_i^s)$, fulfilling $\bar{\mathbf{X}}^s \succeq \mathbf{X}_\infty^s$ and $\bar{\mathbf{D}}^s \succeq \mathbf{D}_\infty^s$. Recalling that $\mathbf{X}_\infty^s \succeq \mathbf{X}^s(t), \forall t \geq 0$, it is evident that $\bar{\mathbf{X}}^s \succeq \mathbf{X}^s(t), \forall t \geq 0$, also holds. Then, the block-wise property $\bar{\mathbf{X}}_i^s \succeq \mathbf{X}_i^s(t), \forall t \geq 0$, is complied for the ith block-diagonal element of $\mathbf{X}^s(t)$ corresponding to the covariance of $\tilde{\mathbf{x}}_i^s(t)$. This can be verified by taking a vector $\mathbf{v}$ containing zeros except for the ith sub-vector, $\mathbf{v}_i$, containing ones, and noting that, since $\bar{\mathbf{X}}^s - \mathbf{X}^s(t) \succeq \mathbf{0}$, we have $0 \leq \mathbf{v}^\top(\bar{\mathbf{X}}^s - \mathbf{X}^s(t))\mathbf{v} = \mathbf{v}_i^\top(\bar{\mathbf{X}}_i^s - \mathbf{X}_i^s(t))\mathbf{v}_i \implies \bar{\mathbf{X}}_i^s - \mathbf{X}_i^s(t) \succeq \mathbf{0}$. Thus, we can use each block-element $\bar{\mathbf{X}}_i^s$ as a uniform covariance upper bound to construct the confidence set for $\tilde{\mathbf{x}}_i^s(t)$ at node i. By the same arguments, the corresponding block element $\bar{\mathbf{D}}_i^s$ for each node i can be used as the uniform covariance upper bound for the disturbance $\mathbf{d}_i^s(m|k)$.

We can now define bounded confidence sets as follows.

Lemma 3: Let Assumptions 1 to 4 hold. Consider the variables $\tilde{\mathbf{x}}_i^s(t) \sim \mathcal{N}(\mathbf{0}, \mathbf{X}_i^s(t))$ and $\mathbf{d}_i^s(m|k) \sim \mathcal{N}(\mathbf{0}, \mathbf{D}_i^s(m|k))$, given for all nodes $i \in \mathcal{V}$ by the stacked dynamics (12b)-(13) and (17b)-(18), respectively. Define the sets $\mathcal{S}_{1-p_x}^{\tilde{\mathbf{x}}_i^s}$ and $\mathcal{S}_{1-p_f}^{\mathbf{d}_i^s}$ according to Lemma 1 with the covariance upper bounds $\bar{\mathbf{X}}_i^s$ and $\bar{\mathbf{D}}_i^s$, where $\bar{\mathbf{X}}_i^s \succeq \mathbf{X}_i^s(t)$, $\forall t$, and $\bar{\mathbf{D}}_i^s \succeq \mathbf{D}_i^s(m|k)$, $\forall m, k$. Then, $\mathbb{P}\{\tilde{\mathbf{x}}_i^s(t) \in \mathcal{S}_{1-p_x}^{\tilde{\mathbf{x}}_i}\} \geq 1 - p_x,\ \forall t$, and $\mathbb{P}\{\mathbf{d}_i^s(m|k) \in \mathcal{S}_{1-p_f}^{\mathbf{d}_i}\} \geq 1 - p_f,\ \forall m, k$.

Proof: The proof follows directly from using Lemma 1 and Definition 1. ■

The following result summarizes the design of bounded confidence sets for $\tilde{\mathbf{x}}_i(t)$ and $\mathbf{d}_i(m|k)$, taking into account their deterministic and stochastic components.

Corollary 1: Let Assumptions 1 to 4 hold and consider the sets defined in Lemmas 2 and 3. Letting $\mathcal{S}^{\tilde{\mathbf{x}}_i}_{1-p_x} = \mathcal{S}^{\tilde{\mathbf{x}}^s_i}_{1-p_x} \oplus \mathcal{S}^{\tilde{\mathbf{x}}^d_i}$, $\mathcal{S}^{\mathbf{d}_i}_{1-p_f} = \mathcal{S}^{\mathbf{d}^s_i}_{1-p_f} \oplus \mathcal{S}^{\mathbf{d}^d_i}$, we have that the estimation error $\tilde{\mathbf{x}}_i(t)$ given by (11) and the disturbance $\mathbf{d}_i(m|k)$ in the control error dynamics (15) fulfill $\mathbb{P}\{\tilde{\mathbf{x}}_i(t) \in \mathcal{S}^{\tilde{\mathbf{x}}_i}_{1-p_x}\} \geq 1-p_x,\ \forall t$, and $\mathbb{P}\{\mathbf{d}_i(m|k) \in \mathcal{S}^{\mathbf{d}_i}_{1-p_f}\} \geq 1-p_f,\ \forall m,k$.

Proof: The proof follows from noting that $\tilde{\mathbf{x}}_i(t) = \tilde{\mathbf{x}}^d_i(t) + \tilde{\mathbf{x}}^s_i(t)$, where $\tilde{\mathbf{x}}^d_i(t) \in \mathcal{S}^{\tilde{\mathbf{x}}^d_i}\ \forall t$ and $\tilde{\mathbf{x}}^s_i(t) \in \mathcal{S}^{\tilde{\mathbf{x}}^s_i}_{1-p_x}$ with probability no less than $1-p_x$. Similarly, $\mathbf{d}_i(m|k) = \mathbf{d}^d_i(m|k) + \mathbf{d}^s_i(m|k)$, where $\mathbf{d}^d_i(m|k) \in \mathcal{S}^{\mathbf{d}^d_i}\ \forall m,k$, and $\mathbf{d}^s_i(m|k) \in \mathcal{S}^{\mathbf{d}^s_i}_{1-p_f}$ with probability no less than $1-p_f$. ■

Remark 3: The size of the sets designed in Lemmas 2 and 3 is influenced by the system matrices and by several design parameters. Note that h and $\delta_{\max}$ are often set to small values (i.e. $h, \delta_{\max} \ll 1$) to keep the discretization and event-triggered errors small. The gain κ does not need to take very high values in practice to fulfill Assumption 3, as seen in the experiments from previous works [23], [25]. The main source of conservativeness in our approach comes from the approximation used in (19). Here, we have assumed the worst case where the input computed at each node is as different as possible from the actual input being applied by other nodes. In Section VI, we discuss alternatives to reduce the conservativeness from this choice.

E. Constraint Tightening

Now, we tighten the sets $\mathcal{X}, \mathcal{U}$ into $\mathcal{Z}_{i,m}, \mathcal{C}_{i,m}$ for the nominal $\mathbf{z}_i(m|k)$, $\mathbf{c}_i(m|k)$ using the previously designed sets. First, we tighten $\mathcal{X}$ to account for the state estimation error $\tilde{\mathbf{x}}_i(t)$ at node i,

$$\hat{\mathcal{X}}_i = \mathcal{X} \ominus \mathcal{S}^{\tilde{\mathbf{x}}_i}_{1-p_x}, \tag{21}$$

recalling the set $\mathcal{S}^{\tilde{\mathbf{x}}^s_i}_{1-p_x}$ defined in Corollary 1. Then, we use a shrinking-tube approach to construct the constraints of the predicted state along the prediction horizon. In this case, we take into account the set $\mathcal{S}^{\mathbf{d}_i}_{1-p_f}$ defined Corollary 1 for the disturbance $\mathbf{d}_i(m|k)$, so that the loss of feasibility is regulated with probability p_f:

$$\begin{aligned} &\mathcal{Z}_{i,0} = \hat{\mathcal{X}}_i, \\ &\mathcal{Z}_{i,m} = \hat{\mathcal{X}}_i \ominus \textstyle\bigoplus_{q=0}^{m-1} \mathbf{A}^q_{\mathsf{cl}} \mathcal{S}^{\mathbf{d}_i}_{1-p_f}, \quad m = 1,\dots,T-1. \end{aligned} \tag{22}$$

Similarly, we tighten the input constraint as follows:

$$\begin{aligned} &\mathcal{C}_{i,0} = \mathcal{U}, \\ &\mathcal{C}_{i,m} = \mathcal{U} \ominus \textstyle\bigoplus_{q=0}^{m-1} \mathbf{L}\mathbf{A}^q_{\mathsf{cl}} \mathcal{S}^{\mathbf{d}_i}_{1-p_f}, \quad m = 1,\dots,T-1. \end{aligned} \tag{23}$$

Note that the resulting constraints may be different for each node i, as the error dynamics of each depend on the local matrices $\mathbf{C}_i, \mathbf{V}_i$ and the neighbor dynamics.

F. Terminal Set

Finally, we design the terminal set $\mathcal{Z}_{i,f}$ to be used in the constraint (9e) of the optimization problem. First, the terminal set must be a positive invariant set under a local stabilizing control law $\mathbf{u}(k) = \mathbf{f}(\mathbf{x}(k))$, for which the constraints are fulfilled for any $\mathbf{x}(k)$ in the set [28, Section 5]. Due to the presence of disturbances in our setup, recall the definition of a robust positive invariant set, used in robust MPC.

Definition 2 ([29]): A set $\mathcal{S} \subseteq \mathcal{X}$ is a robust positive invariant set for an autonomous system $\mathbf{x}(k+1) = \mathbf{A}\mathbf{x}(k) + \mathbf{w}(k)$ subject to $\mathbf{x}(k) \in \mathcal{X}$, $\mathbf{w}(k) \in \mathcal{W}$, where $\mathcal{X}, \mathcal{W}$ are polytopes, if $\mathbf{x}(k) \in \mathcal{S} \implies \mathbf{x}(k+1) \in \mathcal{S}, \forall \mathbf{w}(k) \in \mathcal{W}$.

We consider a control law $\mathbf{u}^*_i(k) = \mathbf{L}\hat{\mathbf{x}}_i(k)$, which stabilizes the system due to our choice of $\mathbf{L}$ in Section III-B. Under this controller, the estimator dynamics (14) can be written as follows, using similar manipulations as before and recalling the variable $\mathbf{d}_i(k)$ defined in the control error dynamics (15),

$$\hat{\mathbf{x}}_i(k+1) = \mathbf{A}_{\mathsf{cl}}\hat{\mathbf{x}}_i(k) + \mathbf{d}_i(k), \tag{24}$$

where $\mathbf{d}_i(k) \in \mathcal{S}^{\mathbf{d}_i}_{1-p_f}$ with probability no less than p_f, according to Corollary 1. For our terminal set, we first construct a robust positively invariant set $\hat{\mathcal{X}}_{i,f} \subseteq \hat{\mathcal{X}}_i$ for the system (24) with $\mathbf{d}_i(k) \in \mathcal{S}^{\mathbf{d}_i}_{1-p_f}$. Thus, according to Definition 2, we design $\hat{\mathcal{X}}_{i,f}$ such that $\hat{\mathbf{x}}_i(k) \in \hat{\mathcal{X}}_{i,f} \implies \hat{\mathbf{x}}_i(k+1) \in \hat{\mathcal{X}}_{i,f}, \forall \mathbf{d}_i(k) \in \mathcal{S}^{\mathbf{d}_i}_{1-p_f}$. In addition, the terminal set must satisfy the input constraint, i.e. $\mathbf{L}\hat{\mathbf{x}}_i \in \mathcal{U}$, $\forall \hat{\mathbf{x}}_i \in \hat{\mathcal{X}}_{i,f}$. Then, we tighten the set $\hat{\mathcal{X}}_{i,f}$ as in the previous section:

$$\mathcal{Z}_{i,f} = \hat{\mathcal{X}}_{i,f} \ominus \textstyle\bigoplus_{q=0}^{T-1} \mathbf{A}^q_{\mathsf{cl}} \mathcal{S}^{\mathbf{d}_i}_{1-p_f}. \tag{25}$$

Second, we require that the terminal set and terminal cost fulfill the following assumption, which is commonly used in MPC literature to ensure that the optimal cost is a Lyapunov function for the system, in order to prove convergence of the system to the steady state [28].

Assumption 5: The terminal set yields the cost decrease

$$\|\mathbf{A}_{\mathsf{cl}}\mathbf{z}\|^2_{\mathbf{Q}_f} - \|\mathbf{z}\|^2_{\mathbf{Q}_f} \leq -\|\mathbf{z}\|^2_{\mathbf{Q}} - \|\mathbf{L}\mathbf{z}\|^2_{\mathbf{R}},\ \forall \mathbf{z} \in \mathcal{Z}_{i,f}. \tag{26}$$

Remark 4: While we have designed the tightened constraint sets to ensure a given probability of recursive feasibility, infeasibility may still occur due to the unbounded disturbances. In such cases, an auxiliary control strategy can be implemented by temporarily removing the state constraint (the one with less fulfillment priority, since its violation is admissible). The auxiliary controller then aims to find inputs that respect the hard input constraint while steering the state towards the origin. Note that the backup strategies in other SMPC works, e.g. [3], [16], [22], cannot be used, as they may violate the input constraint.

V. Properties of the SMPC Controller

In this section, we derive the recursive feasibility, constraint satisfaction and stability properties of the designed output-feedback distributed SMPC controller. While the proofs for recursive feasibility and constraint satisfaction in [6] are relevant, note that the complexity of extending that proof structure to the distributed case lies in appropriately designing the disturbance sets. As detailed in Section IV, the distributed case requires the consideration of aspects such as coupling-induced errors, the effect of having distributed control inputs which are unknown from each node, or the disturbances caused by event-triggered communication. Moreover, we guarantee stability for our proposal, which was omitted from [6].

A. Probabilistic Recursive Feasibility

First, we show recursive feasibility of the optimization problem solved by each actuator node with no less than a desired user-defined probability $1-p_f$.

Theorem 1: Let Assumptions 1 to 4 hold. Consider the closed loop system (3) along with the inputs computed by the MPC (9), initialized with the estimates from (5) and with constraints (22), (23), (25). Then, if the optimization problem at node i is feasible at step k, it is feasible at step $k+1$ with probability no less than $1-p_f$.

Proof: We prove recursive feasibility of the optimization problem (9) when $\mathbf{d}_i(k) \in \mathcal{S}^{\mathbf{d}_i}_{1-p_f}$, recalling that $\mathbb{P}\{\mathbf{d}_i(m|k) \in \mathcal{S}^{\mathbf{d}_i}_{1-p_f}\} \geq 1-p_f$, according to Corollary 1. Considering $\mathbf{z}_i(0|k) = \hat{\mathbf{x}}_i(k)$ and the nominal dynamics (8), the estimator dynamics can be rewritten as

$$\begin{aligned}\hat{\mathbf{x}}_i(k+1) &= \mathbf{A}_{\mathsf{d}}\hat{\mathbf{x}}_i(k) + \mathbf{B}_{\mathsf{d}}\hat{\mathbf{u}}_i(k) + \mathbf{d}_i(k)\\ &= \mathbf{A}_{\mathsf{d}}\mathbf{z}_i(0|k) + \mathbf{B}_{\mathsf{d}}\mathbf{c}_i(0|k) + \mathbf{d}_i(k) = \mathbf{z}_i(1|k) + \mathbf{d}_i(k),\end{aligned} \tag{27}$$

recalling that $\hat{\mathbf{u}}_i(k) = \mathbf{c}_i(0|k)$ since $\mathbf{e}_i(0|k) = \mathbf{0}$ in (7). Consider the following candidate solution for the MPC at step $k+1$, taking into account the optimal solution computed at time k:

$$\tilde{\mathbf{c}}_i(m|k+1) = \begin{cases}\mathbf{c}_i(m+1|k) + \mathbf{L}\mathbf{A}_{\mathsf{cl}}^m\mathbf{d}_i(k), \\ \qquad\qquad m = 0,\dots,T-2,\\ \mathbf{L}(\mathbf{z}_i(T|k) + \mathbf{A}_{\mathsf{cl}}^m\mathbf{d}_i(k)),\ m = T-1.\end{cases} \tag{28}$$

Then, the nominal states at step $k+1$, considering (28) and the initialization to $\hat{\mathbf{x}}_i(k+1)$ which fulfills (27), are:

$$\mathbf{z}_i(m|k+1) = \begin{cases}\mathbf{z}_i(m+1|k) + \mathbf{A}_{\mathsf{cl}}^m\mathbf{d}_i(k),\\ \qquad\qquad m = 0,\dots,T-1,\\ \mathbf{A}_{\mathsf{cl}}\mathbf{z}_i(T-1|k+1),\ m = T.\end{cases} \tag{29}$$

To show that the problem remains feasible at $k+1$, we prove that the candidate solution (28)-(29) fulfills $\mathbf{z}_i(m|k+1) \in \mathcal{Z}_{i,m},\ \tilde{\mathbf{c}}_i(m|k+1) \in \mathcal{C}_{i,m}$, for $m = 0,\dots,T$.

First, according to [30, Lemma 7], the candidate solution fulfills $\tilde{\mathbf{c}}_i(m|k+1) \in \mathcal{C}_{i,m},\ \mathbf{z}_i(m|k+1) \in \mathcal{Z}_{i,m}$ for $i = 0,1,\dots,T-2$. Now, we verify that $\tilde{\mathbf{c}}_i(m|k+1)$ fulfills the constraint as well for $m = T-1$:

$$\begin{aligned}&\mathbf{z}_i(T|k) \in \mathcal{Z}_{i,f}\\ &\implies \mathbf{z}_i(T|k) + \textstyle\sum_{q=0}^{T-1}\mathbf{A}_{\mathsf{cl}}^q\mathbf{d}_i(q) \in \hat{\mathcal{X}}_{i,f},\ \forall \mathbf{d}_i(q) \in \mathcal{S}^{\mathbf{d}_i}_{1-p_f}\\ &\implies \mathbf{L}(\mathbf{z}_i(T|k) + \textstyle\sum_{q=0}^{T-1}\mathbf{A}_{\mathsf{cl}}^q\mathbf{d}_i(q)) \in \mathcal{U},\ \forall \mathbf{d}_i(q) \in \mathcal{S}^{\mathbf{d}_i}_{1-p_f}\\ &\implies \underbrace{\mathbf{L}(\mathbf{z}_i(T|k) + \mathbf{A}_{\mathsf{cl}}^{T-1}\mathbf{d}_i(k))}_{\tilde{\mathbf{c}}_i(T-1|k+1)\ \because\ (28)} \in \underbrace{\mathcal{U} \ominus \textstyle\bigoplus_{q=0}^{T-2}\mathbf{L}\mathbf{A}_{\mathsf{cl}}^q\mathcal{S}^{\mathbf{d}_i}_{1-p_f}}_{\mathcal{C}_{i,T-1}\ \because\ (23)}.\end{aligned}$$

The second implication results from the fact that $\mathbf{L}\mathbf{x} \in \mathcal{U},\ \forall \mathbf{x} \in \hat{\mathcal{X}}_{i,f}$ by design of the terminal set in Section IV-F. Next, we show that $\mathbf{z}_i(T|k) \in \mathcal{Z}_{i,f}$ implies that the state at next time step fulfills $\mathbf{z}_i(T-1|k+1) \in \mathcal{Z}_{i,T-1}$:

$$\begin{aligned}&\mathbf{z}_i(T|k) \in \mathcal{Z}_{i,f}\\ &\implies \mathbf{z}_i(T|k) + \textstyle\sum_{q=0}^{T-1}\mathbf{A}_{\mathsf{cl}}^q\mathbf{d}_i(q) \in \hat{\mathcal{X}}_{i,f},\ \forall \mathbf{d}_i(q) \in \mathcal{S}^{\mathbf{d}_i}_{1-p_f}\\ &\implies \mathbf{z}_i(T|k) + \mathbf{A}_{\mathsf{cl}}^{T-1}\mathbf{d}_i(k) \in \hat{\mathcal{X}}_{i,f} \ominus \textstyle\bigoplus_{q=0}^{T-2}\mathbf{A}_{\mathsf{cl}}^q\mathcal{S}^{\mathbf{d}_i}_{1-p_f}\\ &\implies \underbrace{\mathbf{z}_i(T|k) + \mathbf{A}_{\mathsf{cl}}^{T-1}\mathbf{d}_i(k)}_{\mathbf{z}_i(T-1|k+1)\ \because\ (29)} \in \underbrace{\hat{\mathcal{X}}_i \ominus \textstyle\bigoplus_{q=0}^{T-2}\mathbf{A}_{\mathsf{cl}}^q\mathcal{S}^{\mathbf{d}_i}_{1-p_f}}_{\mathcal{Z}_{i,T-1}\ \because\ (22)},\end{aligned}$$

recalling that $\hat{\mathcal{X}}_{i,f} \subseteq \hat{\mathcal{X}}_i$, which we have used in the last line. Finally, for $i = T$, we have

$$\begin{aligned}&\mathbf{z}_i(T|k) \in \mathcal{Z}_{i,f}\\ &\implies \mathbf{z}_i(T|k) + \textstyle\sum_{q=0}^{T-1}\mathbf{A}_{\mathsf{cl}}^q\mathbf{d}_i(q) \in \hat{\mathcal{X}}_{i,f},\ \forall \mathbf{d}_i(q) \in \mathcal{S}^{\mathbf{d}_i}_{1-p_f}\\ &\implies \mathbf{A}_{\mathsf{cl}}\mathbf{z}_i(T|k) + \textstyle\sum_{q=0}^{T}\mathbf{A}_{\mathsf{cl}}^q\mathbf{d}_i(q) \in \hat{\mathcal{X}}_{i,f},\ \forall \mathbf{d}_i(q) \in \mathcal{S}^{\mathbf{d}_i}_{1-p_f}\\ &\implies \underbrace{\mathbf{A}_{\mathsf{cl}}(\mathbf{z}_i(T|k) + \mathbf{A}_{\mathsf{cl}}^{T-1}\mathbf{d}_i(k))}_{\mathbf{z}_i(T|k+1)\ \because\ (29)} \in \underbrace{\hat{\mathcal{X}}_{i,f} \ominus \textstyle\bigoplus_{q=0}^{T-1}\mathbf{A}_{\mathsf{cl}}^q\mathcal{S}^{\mathbf{d}_i}_{1-p_f}}_{\mathcal{Z}_{i,f}\ \because\ (25)},\end{aligned}$$

where the second implication follows from $\hat{\mathcal{X}}_{i,f}$ being a robust positive invariant set. This completes the proof of recursive feasibility showing that the candidate sequence (28) based on the solution at time k is a feasible solution for the next step $k+1$, with no less than the desired probability level $1-p_f$. ■

B. Closed-Loop Constraint Satisfaction

Next, we show that feasibility of the optimization problem over the nominal states and inputs $\mathbf{z}_i(m|k)$, $\mathbf{c}_i(m|k)$ also implies the closed-loop constraint satisfaction for the states and inputs $\mathbf{x}(k)$, $\mathbf{u}(k)$ under stochastic disturbances.

Theorem 2: Let Assumptions 1 to 4 hold. If the MPC (9), initialized with the estimates from (5) and with constraints (22), (23), (25), is feasible at time step k, then the constraints (4) are satisfied in closed loop.

Proof: First, we show that $\mathbb{P}\{\mathbf{x}(k) \in \mathcal{X}\} \geq 1-p_x$ is fulfilled. Due to the initialization $\mathbf{z}_i(0|k) = \hat{\mathbf{x}}_i(k)$, we have $\mathbf{z}_i(0|k) \in \mathcal{Z}_{i,0} \iff \hat{\mathbf{x}}_i(k) \in \mathcal{Z}_{i,0} = \hat{\mathcal{X}}_i$. Note that $\mathbf{x}(k) - \hat{\mathbf{x}}_i(k) = \tilde{\mathbf{x}}_i(k)$. According to Corollary 1, $\mathbb{P}\{\mathbf{x}(k) - \hat{\mathbf{x}}_i(k) \in \mathcal{S}^{\tilde{\mathbf{x}}_i}_{1-p_x}\} \geq 1-p_x$. Then, $\hat{\mathbf{x}}_i(k) \in \hat{\mathcal{X}}_i$, with $\hat{\mathcal{X}}_i$ as in (21), implies $\mathbb{P}\{\mathbf{x}(k) \in \mathcal{X}\} \geq 1-p_x$.

Now, we prove $\mathbf{u}(k) \in \mathcal{U}$. Note that $\mathbf{e}_i(0|k) = \hat{\mathbf{x}}_i(k) - \mathbf{z}_i(0|k) = \mathbf{0}$ in (7) and therefore the computed control input at node i fulfills $\hat{\mathbf{u}}_i(k) = \mathbf{c}_i(0|k) \in \mathcal{C}_{i,0} = \mathcal{U}$. Recalling that $\mathcal{U} = \mathcal{U}_1 \times \cdots \times \mathcal{U}_N$, this implies that $\hat{\mathbf{u}}_{i,j} \in \mathcal{U}_j,\ \forall i,j \in \mathcal{V}$, i.e. each of the inputs computed by each node fulfills the constraints for each of the actuators. Then, node i applies the elements of $\hat{\mathbf{u}}_i(k)$ corresponding to the ith actuator in closed loop, as $\mathbf{u}_i(k) = \hat{\mathbf{u}}_{i,i}(k)$. Since $\hat{\mathbf{u}}_i(k) \in \mathcal{U}_i,\ \forall i \in \mathcal{V}$, it follows that $\mathbf{u}(k) = \mathsf{col}_{i=1}^N(\hat{\mathbf{u}}_{i,i}(k)) \in \mathcal{U}$, completing the proof. ■

C. Convergence

Note that, due to the persistent stochastic disturbances that affect the system, the state will not converge to the origin but rather remain in a region around it, with a bounded error covariance. To show a notion of stability for our SMPC proposal, we first show the decrease of the optimal cost of (9) from step k to $k+1$, and then we provide an average asymptotic cost bound, similarly to the approach of [3], [22]. In addition, due to the stochastic noises and the hard input constraints considered in this work, some noise realizations can result in values of $\hat{\mathbf{x}}_i(t)$ that render the optimization problem (9) infeasible. Recalling the result in Theorem 1, the problem remains feasible at the next step with probability $1-p_f$. Then, as long as the optimization problem remains feasible, the following convergence results hold. We make the following additional assumption:

Assumption 6: There is a bounded set of estimates $\hat{\mathbf{x}}_i(k)$ for which the optimization problem (9) is feasible.

Assumption 6 holds for bounded terminal and input constraint sets, which is the usual case. Now, we can state our convergence results.

Lemma 4: Let Assumptions 1 to 6 hold. Consider system (3) along with the control law (7) computed by the MPC controller (9) using the estimates from (5). Let $J^*(\hat{\mathbf{x}}_i(k))$ be the optimal cost (9a) for the optimization problem. If the problem is feasible at $k+1$, we have

$$\begin{aligned}&\mathbb{E}\{J^*(\hat{\mathbf{x}}_i(k+1))\} - J^*(\hat{\mathbf{x}}_i(k))\\&\le -\|\hat{\mathbf{x}}_i(k)\|^2_{\mathbf{Q}} - \|\hat{\mathbf{u}}_i(k)\|^2_{\mathbf{R}} + \alpha D^d + \alpha\sqrt{\mathrm{tr}(\bar{\mathbf{D}}^s_i)},\end{aligned} \tag{30}$$

where α is a Lipschitz constant.

Proof: In the following, we consider the optimization problem (9) at an arbitrary node i. Let $J(\mathbf{z},\mathbb{C})$ denote the cost (9a) for a sequence of inputs $\mathbb{C}$ with initial state $\mathbf{z}$. Note that the optimal cost $J^*(\mathbf{z})$ of a nominal MPC with a quadratic cost function is known to be piecewise quadratic in $\mathbf{z}$ [31]. Along with Assumption 6, this implies the existence of a Lipschitz constant α such that

$$J^*(\mathbf{z}+\mathbf{e}) \le J^*(\mathbf{z}) + \alpha\|\mathbf{e}\|.$$

The expected cost for step $k+1$, conditioned on feasibility of the optimization problem, can be evaluated as follows:

$$\begin{aligned}&\mathbb{E}\{J^*(\hat{\mathbf{x}}_i(k+1))\} = \mathbb{E}\{J^*(\mathbf{z}_i(1|k)+\mathbf{e}_i(1|k))\}\\&\quad\le J^*(\mathbf{z}_i(1|k)) + \alpha\mathbb{E}\{\|\mathbf{e}_i(1|k)\|\}\\&\quad\le J(\mathbf{z}_i(1|k),\bar{\mathbb{C}}_i) + \alpha\mathbb{E}\{\|\mathbf{e}_i(1|k)\|\},\end{aligned}$$

where $\bar{\mathbb{C}}_i = \{\mathbf{c}_i(1|k),\ldots,\mathbf{c}_i(T-1|k),\mathbf{L}\mathbf{z}_i(T|k)\}$ represents the shifted solution, i.e. applying the inputs computed by node i from the optimization at the previous step k. The last inequality is due to the shifted solution being feasible but suboptimal compared to $J^*(\mathbf{z}_i(1|k))$. Considering (15), we can further evaluate

$$\begin{aligned}&\mathbb{E}\{\|\mathbf{e}_i(1|k)\|\} = \mathbb{E}\{\|\mathbf{d}_i(0|k)\|\}\\&\quad\le \|\mathbf{d}^d_i(0|k)\| + \mathbb{E}\{\|\mathbf{d}^s_i(0|k)\|\} \le D^d + \sqrt{\mathrm{tr}(\bar{\mathbf{D}}^s_i)},\end{aligned}$$

recalling that $\mathbf{d}_i(m|k)$ can be split into a deterministic part $\mathbf{d}^d_i(m|k)$, fulfilling $\|\mathbf{d}^d_i(m|k)\| \le D^d$, and a stochastic part $\mathbf{d}^s_i(m|k)$ with zero mean and covariance bounded by $\bar{\mathbf{D}}^s_i$, as explained in Sections IV-C and IV-D. Now, we evaluate the following cost difference:

$$\begin{aligned}&\mathbb{E}\{J^*(\hat{\mathbf{x}}_i(k+1))\} - J^*(\hat{\mathbf{x}}_i(k))\\&\le J(\mathbf{z}_i(1|k),\bar{\mathbb{C}}_i) + \alpha D^d + \alpha\sqrt{\mathrm{tr}(\bar{\mathbf{D}}^s_i)} - J^*(\hat{\mathbf{x}}_i(k)).\end{aligned} \tag{31}$$

Note that

$$\begin{aligned}&J(\mathbf{z}_i(1|k),\bar{\mathbb{C}}_i) - J^*(\hat{\mathbf{x}}_i(k))\\&= \|\mathbf{A}_{\mathsf{cl}}\mathbf{z}_i(T|k)\|^2_{\mathbf{Q}_f} + \|\mathbf{z}_i(T|k)\|^2_{\mathbf{Q}} + \|\mathbf{L}\mathbf{z}_i(T|k)\|^2_{\mathbf{R}}\\&\quad - \|\mathbf{z}_i(T|k)\|^2_{\mathbf{Q}_f} - \|\mathbf{z}_i(0|k)\|^2_{\mathbf{Q}} - \|\mathbf{c}_i(0|k)\|^2_{\mathbf{R}}\\&\le -\|\mathbf{z}_i(0|k)\|^2_{\mathbf{Q}} - \|\mathbf{c}_i(0|k)\|^2_{\mathbf{R}} = -\|\hat{\mathbf{x}}_i(k)\|^2_{\mathbf{Q}} - \|\hat{\mathbf{u}}_i(k)\|^2_{\mathbf{R}},\end{aligned} \tag{32}$$

due to $J(\mathbf{z}_i(1|k),\bar{\mathbb{C}}_i)$ using the shifted solution from step k, and recalling the property (26) of the terminal controller. Substituting (32) into (31), we reach (30), completing the proof. ■

Theorem 3: Let Assumptions 1 to 6 hold. Consider system (3) along with the control law (7) computed by the MPC controller (9) and with the estimates from (5). If the optimization problem remains feasible, which occurs with probability no less than $1-p_f$ at each step, we have

$$\lim_{q\to\infty}\frac{1}{q}\sum_{k=0}^{q}\mathbb{E}\{\|\hat{\mathbf{x}}_i(k)\|^2_{\mathbf{Q}} + \|\hat{\mathbf{u}}_i(k)\|^2_{\mathbf{R}}\} \le D', \tag{33}$$

with $D' = \alpha D^d + \alpha\sqrt{\mathrm{tr}(\bar{\mathbf{D}}^s_i)}$.

Proof: Taking the optimal cost as a stochastic Lyapunov function, and using the result from Lemma 4 in the second inequality, yields:

$$\begin{aligned}&\lim_{q\to\infty}\frac{1}{q}\mathbb{E}\{J^*(\hat{\mathbf{x}}_i(q)) - J^*(\hat{\mathbf{x}}_i(0))\}\\&\le \lim_{q\to\infty}\frac{1}{q}\sum_{k=0}^{q}\mathbb{E}\{J^*(\hat{\mathbf{x}}_i(k+1)) - J^*(\hat{\mathbf{x}}_i(k))\}\\&\le \lim_{q\to\infty}\frac{1}{q}\sum_{k=0}^{q}\mathbb{E}\{-\|\hat{\mathbf{x}}_i(k)\|^2_{\mathbf{Q}} - \|\hat{\mathbf{u}}_i(k)\|^2_{\mathbf{R}}\} + D'.\end{aligned} \tag{34}$$

Then, using similar arguments as [32, Theorem 6], the result (33) follows. ■

Remark 5: Theorem 3 provides a bound for the average asymptotic cost, which is dependent on the magnitude of the disturbances. As shown in its proof, the limit (34) is non-positive when the cost is high, and therefore $J^*(\hat{\mathbf{x}}(k))$ decreases "on average" along the trajectories of the process. When the cost is small, the limit (34) becomes positive and the cost increases on the average. Therefore, the disturbances cause the expected value of the states and inputs to remain in a compact set around the origin.

VI. Simulation Experiments

We show an illustrative simulation example to validate our proposal. In addition, we discuss the main source of conservativeness in our approach, showing that it can be reduced while maintaining a satisfactory performance.

The plant to be controlled has a state vector $\mathbf{x}(t) = [x_1(t), x_2(t), x_3(t)]^\top$, with dynamics given by (2) with

$$\mathbf{A} = \begin{bmatrix}0&1&0\\0&0&1\\0&0&0\end{bmatrix},\quad \mathbf{B} = \begin{bmatrix}1&0&0\\0&1&0\\-1&0&1\end{bmatrix},$$
$$\mathbf{W} = \begin{bmatrix}0.1&0.001&0\\0.001&0.1&0.001\\0&0.001&0.1\end{bmatrix}.$$

The initial state is $\mathbf{x}_0 = 3\mathbb{1}_N$, $\mathbf{P}_0 = 0.01\mathbf{I}_N$. The plant is controlled by $N=3$ actuator nodes, which have scalar inputs

TABLE I: Average result comparison for 1000 simulations.

Method	Average cost J	Communication rate C
Centralized, [6]	13.617	-
Ours, $\delta_i = 0$	13.851	1
Ours, $\delta_i = 0.01$	14.159	0.153
Ours, $\delta_i = 0.01$, $U = 0$	14.158	0.154

$u_i(t)$. The measurements for each node are given by (1b) with $\mathbf{C}_1 = [1, 0, 0]$, $\mathbf{C}_2 = [0, 1, 0]$, $\mathbf{C}_3 = [0, 0, 1]$, and $\mathbf{V}_i = 0.01, \forall i \in \mathcal{V}$. The communication neighbors of each node are given by $\mathcal{N}_1 = \{2\}$, $\mathcal{N}_2 = \{1, 3\}$, $\mathcal{N}_3 = \{2\}$. The state and input sets are $\mathcal{X} = \{\mathbf{x} \in \mathbb{R}^N : -5\mathbb{1}_N \leq \mathbf{x} \leq 5\mathbb{1}_N\}$, $\mathcal{U} = \{\mathbf{u} \in \mathbb{R}^N : -5\mathbb{1}_N \leq \mathbf{u} \leq 5\mathbb{1}_N\}$. We set $p_x = 0.5$ for the state constraint in (4) and $p_f = 0.99$ in this example. The system dynamics have been approximated in simulation using the Euler-Maruyama method with simulation step $h = 10^{-3}$s. The optimal control problem is also solved with step h. In addition, we set $\underline{\tau} = h$ as the minimum inter-event time in (6). We set $\kappa = 10000$ for the state estimator (5). In this example, each node solves (9) with horizon $T = 5$ steps and weighting cost matrices $\mathbf{Q} = \mathbf{I}_N$, $\mathbf{R} = \mathbf{I}_N$. The weight $\mathbf{Q}_f$ for the terminal cost has been set as the solution to the discrete-time Riccati equation for the unconstrained infinite-horizon optimal control problem,

$$\begin{aligned}\mathbf{Q}_f = &\, \mathbf{A}_\mathsf{d}^\top \mathbf{Q}_f \mathbf{A}_\mathsf{d} + \mathbf{Q} \\ &- (\mathbf{A}_\mathsf{d}^\top \mathbf{Q}_f \mathbf{B}_\mathsf{d})(\mathbf{R} + \mathbf{B}_\mathsf{d}^\top \mathbf{Q}_f \mathbf{B}_\mathsf{d})^{-1}(\mathbf{B}_\mathsf{d}^\top \mathbf{Q}_f \mathbf{A}_\mathsf{d}),\end{aligned}$$

and with $\mathbf{L} = -(\mathbf{R} + \mathbf{B}_\mathsf{d}^\top \mathbf{Q}_f \mathbf{B}_\mathsf{d})^{-1}(\mathbf{B}_\mathsf{d}^\top \mathbf{Q}_f \mathbf{A}_\mathsf{d})$ being the corresponding optimal control gain. We have used box approximations of the sets to simplify the set-theoretical operations during constraint tightening, as suggested in [33].

We compare our results against the proposal from [6] as a baseline, since it is, to the best of our knowledge, the only work that considers SMPC with hard input constraints. We implement it as a centralized controller. We show our distributed proposal running at full communication, i.e. setting the event threshold $\delta_i = 0$ in (6), and under event-triggered communication with $\delta_i = 0.01$. We compute the average cost J of the sequence and the communication rate C as

$$J = \frac{1}{T_f} \int_0^{T_f} \left(\|\mathbf{x}(\tau)\|^2_{\mathbf{Q}} + \|\mathbf{u}(\tau)\|^2_{\mathbf{R}} \right) \mathrm{d}\tau, \;\; C = \frac{\sum_{i=1}^{N} e_i \, h}{N \, T_f},$$

where T_f is the length of the simulation, which we have set to $T_f = 5$s, and e_i is the number of events triggered at node i. $C = 1$ means full communication, where each node transmits at every simulation step, and $C = 0$ for no communication.

Table I summarizes the average results obtained for 1000 simulations, to account for the stochastic behavior, validating that our distributed SMPC achieves a similar control performance to the centralized baseline. Moreover, using event-triggered communication successfully reduces the communication rate without causing a high impact on performance. Figure 2 shows an example of the state and input trajectories for one simulation, for each option. We have simulated all setups with the same noise realizations of $\mathbf{w}(t)$ and $\mathbf{v}_i(t)$, for a fair comparison. The distributed controller computes similar inputs as the centralized one, despite the dynamical interactions and each actuator node having partial measurement information. The full-communication controller (Fig. 2b) regulates the state closer to the origin in steady state than in the event-triggered case (Fig. 2c), since more information is exchanged. Still, our event-triggered version using only 15% of communication slots achieves similar performance. The centralized input looks noisier than in the distributed case due to having centralized measurements handled by a Kalman filter. In the distributed case, our estimator produces continuous-time estimates which may also be smoother due to the consensus term.

Regarding the disturbance sets $\mathcal{S}^{\tilde{\mathbf{x}}_i}_{1-p_x}$ and $\mathcal{S}^{\mathbf{d}_i}_{1-p_f}$ used for constraint tightening, Figure 3 compares the sets in the centralized and distributed cases. The set related to the state estimation error $\tilde{\mathbf{x}}_i(t)$ is more conservative for the distributed setup than in the centralized case, which is expected since each node has only partial measurement information and is affected by the estimation error dynamics of neighboring nodes. The set related to the control disturbance $\mathbf{d}_i(m|k)$, which is used for the shrinking-tube constraint tightening, is similar for both.

Recalling Remark 3, the worst-case approximation from (19) is the main source of conservativeness in our design. In practice, the consensus-based filter ensures that all nodes hold similar state estimates (especially as κ is increased). Therefore, the estimated inputs $\hat{\mathbf{u}}_i(t)$ should closely resemble $\mathbf{u}(t)$, as all nodes are solving a similar optimization problem based on their estimate. The high level of agreement can be seen in Figure 4. Thus, an option to reduce conservativeness is to disregard this source of error, setting $U = 0$ in (20). The resulting sets are shown in Figure 5 against the original ones. In addition, we included simulations with this configuration in the last row of Table I to verify that a similar performance is still maintained. In order to maintain the safety guarantees, other options can also be explored at the cost of additional transmissions of information, such as sharing the computed input with neighboring nodes, so that they know the input of $|\mathcal{N}_i| + 1$ actuators, or implementing an auxiliary consensus algorithm to estimate the global input.

Finally, our sets for constraint tightening may be more conservative than for other SMPC approaches, due to the consideration of hard input constraints. In addition, we used uniform bounds for the disturbances, which allows to tighten the constraints offline, ensuring that only the state estimates need to be communicated in our setup. Hence, in contrast to approaches based on distributed optimization, our proposal heavily reduces the communication load.

VII. Conclusions

We have proposed an output-feedback distributed SMPC scheme for cooperative control of a plant by several actuator nodes under hard input constraints. In addition, we introduce an event-triggering mechanism to reduce the necessary communication load. In order to deal with the disturbances that affect the system, we design confidence sets containing the disturbances with a desired probability level, through analysis of the joint error dynamics in the distributed setup. By tightening the original constraints according to these confidence sets,

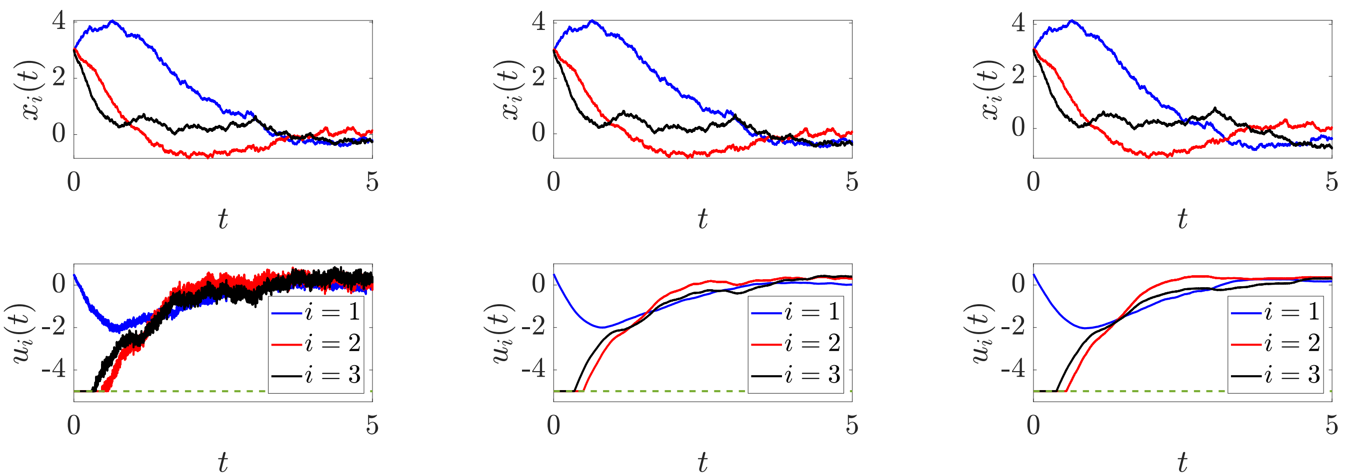

(a) (b) (c)

Fig. 2: Evolution of states and inputs with different controllers: (a) centralized SMPC from [6], (b) our distributed SMPC with full communication, (c) our distributed SMPC under event-triggered communication (only ∼15% of communication is used).

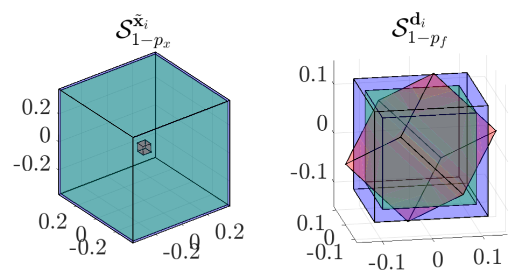

Fig. 3: Disturbance sets. The centralized case from [6] is shown in red, our distributed case with $\delta_i = 0$ in green and with $\delta_i = 0.01$ in blue.

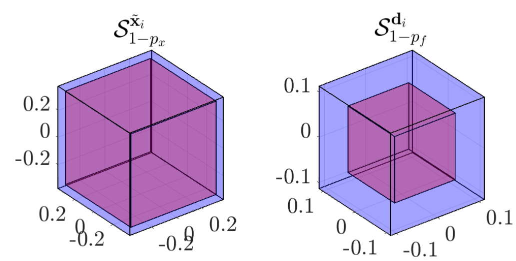

Fig. 5: Comparison of disturbance sets. The distributed case considering the control mismatch $\tilde{\mathbf{u}}(t)$ is in blue, while the case disregarding its effect is in red.

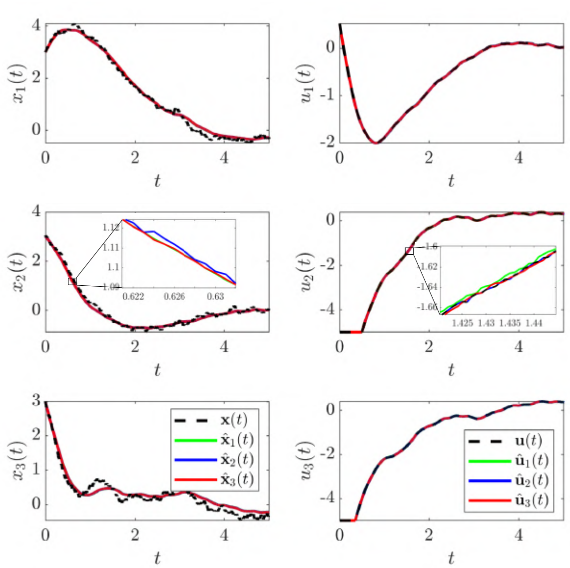

Fig. 4: State and input estimates $\hat{\mathbf{x}}_i(t), \hat{\mathbf{u}}_i(t)$ computed by each actuator node in the distributed case, for each of the state and input components $x_i(t), u_i(t)$.

we ensure the recursive feasibility of the optimization problem with no less than a guaranteed probability, the satisfaction of the probabilistic and hard constraints, and the stability of the system under the proposed SMPC controller. Finally, we have shown through simulation experiments that our distributed SMPC under event-triggered communication achieves similar performance to the centralized and full-communication counterparts, at a fraction of the communication load.

References

[1] A. Mesbah, "Stochastic model predictive control: An overview and perspectives for future research," *IEEE Control Syst.*, vol. 36, pp. 30–44, 2016.

[2] M. Lorenzen, F. Dabbene, R. Tempo, and F. Allgöwer, "Constraint-tightening and stability in stochastic model predictive control," *IEEE Trans. Autom. Control*, vol. 62, no. 7, pp. 3165–3177, 2017.

[3] L. Hewing and M. N. Zeilinger, "Stochastic model predictive control for linear systems using probabilistic reachable sets," in *2018 IEEE Conference on Decision and Control (CDC)*, 2018, pp. 5182–5188.

[4] M. Cannon, Q. Cheng, B. Kouvaritakis, and S. V. Raković, "Stochastic tube MPC with state estimation," *Automatica*, vol. 48, pp. 536–541, 2012.

[5] M. Farina, L. Giulioni, L. Magni, and R. Scattolini, "An approach to output-feedback MPC of stochastic linear discrete-time systems," *Automatica*, vol. 55, pp. 140–149, 2015.

[6] E. Joa, M. Bujarbaruah, and F. Borrelli, "Output feedback stochastic MPC with hard input constraints," in *2023 American Control Conference (ACC)*, 2023, pp. 2034–2039.

[7] S. Muntwiler, K. P. Wabersich, R. Miklos, and M. N. Zeilinger, "LQG for constrained linear systems: Indirect feedback stochastic MPC with Kalman filtering," in *2023 European Control Conference (ECC)*, 2023.

[8] S. Yan, M. Cannon, and P. J. Goulart, "Stochastic output feedback MPC with intermittent observations," *Automatica*, vol. 141, 2022.

[9] M. A. Sehr and R. R. Bitmead, "Particle model predictive control: Tractable stochastic nonlinear output-feedback MPC," *IFAC PapersOnLine*, vol. 50, pp. 15 361–15 366, 2017.

[10] E. Bradford and L. Imsland, "Stochastic nonlinear model predictive control with state estimation by incorporation of the unscented Kalman filter," *IFAC-PapersOnLine*, vol. 51, pp. 417–422, 2018.

[11] L. Dai, Y. Gao, L. Xie, K. H. Johansson, and Y. Xia, "Stochastic self-triggered model predictive control for linear systems with probabilistic constraints," *Automatica*, vol. 92, pp. 9–17, 2018.

[12] Y. Lian, Y. Jiang, N. Stricker, L. Thiele, and C. N. Jones, "Resource-aware stochastic self-triggered model predictive control," *IEEE Control Syst. Lett.*, vol. 6, pp. 1262–1267, 2022.

[13] S. Wildhagen and F. Allgower, "Uncertainties and output feedback in rollout event-triggered control," *IEEE Trans. Control Network Syst.*, vol. 10, pp. 1195–1208, 2023.

[14] C. Gu, X. Wang, A. Yi, and L. Wang, "Event-triggered stochastic MPC for linear systems with additive stochastic disturbances," in *18th IEEE Conference on Industrial Electronics and Applications (ICIEA)*, 2023, pp. 1626–1631.

[15] V. Rostampour and T. Keviczky, "Distributed stochastic model predictive control synthesis for large-scale uncertain linear systems," in *2018 American Control Conference (ACC)*, 2018, pp. 2071–2077.

[16] C. Mark and S. Liu, "Stochastic distributed predictive tracking control under inexact minimization," *IEEE Trans. Control Network Syst.*, vol. 8, pp. 1892–1904, 2021.

[17] S. Muntwiler, K. P. Wabersich, L. Hewing, and M. N. Zeilinger, "Data-driven distributed stochastic model predictive control with closed-loop chance constraint satisfaction," in *2021 European Control Conference (ECC)*, 2021, pp. 210–215.

[18] L. Zhang, B. Wang, Y. Li, and Y. Tang, "Distributed stochastic model predictive control for cyber–physical systems with multiple state delays and probabilistic saturation constraints," *Automatica*, vol. 129, 2021.

[19] S. Lu, X. Wang, L. Wang, L. Jia, M. Shao, and Y. Yu, "Distributed event-trigger model predictive control for stochastic disturbance systems," in *17th IEEE Conference on Industrial Electronics and Applications (ICIEA)*, 2022, pp. 138–143.

[20] J. Chen, H. Wei, H. Zhang, and Y. Shi, "Asynchronous self-triggered stochastic distributed MPC for cooperative vehicle platooning over vehicular ad-hoc networks," *IEEE Trans. Veh. Technol.*, vol. 72, pp. 14 061–14 073, 2023.

[21] L. Dai, Y. Xia, Y. Gao, B. Kouvaritakis, and M. Cannon, "Cooperative distributed stochastic MPC for systems with state estimation and coupled probabilistic constraints," *Automatica*, vol. 61, pp. 89–96, 2015.

[22] C. Mark and S. Liu, "A stochastic output-feedback MPC scheme for distributed systems," in *2020 American Control Conference (ACC)*, 2020, pp. 1937–1942.

[23] I. Perez-Salesa, R. Aldana-Lopez, and C. Sagues, "Event-triggered distributed state estimation based on asymptotic Kalman-Bucy filter," in *22nd European Control Conference (ECC24)*, 2024.

[24] X. Ge, Q. L. Han, X. M. Zhang, and D. Ding, "Dynamic event-triggered control and estimation: A survey," *Int. J. Autom. Comput.*, vol. 18, no. 6, pp. 857–886, 2021.

[25] S. Battilotti, F. Cacace, M. d'Angelo, and A. Germani, "Asymptotically optimal consensus-based distributed filtering of continuous-time linear systems," *Automatica*, vol. 122, 12 2020.

[26] D. Mayne, M. Seron, and S. Raković, "Robust model predictive control of constrained linear systems with bounded disturbances," *Automatica*, vol. 41, no. 2, pp. 219–224, 2005.

[27] M. Farina, L. Giulioni, and R. Scattolini, "Distributed predictive control of stochastic linear systems with chance constraints," in *2016 American Control Conference (ACC)*, 2016, pp. 20–25.

[28] E. F. Camacho and C. Bordons, *Nonlinear Model Predictive Control: An Introductory Review*. Berlin, Heidelberg: Springer Berlin Heidelberg, 2007, pp. 1–16.

[29] F. Borrelli, A. Bemporad, and M. Morari, *Predictive Control for Linear and Hybrid Systems*. Cambridge University Press, 2017.

[30] L. Chisci, J. Rossiter, and G. Zappa, "Systems with persistent disturbances: predictive control with restricted constraints," *Automatica*, vol. 37, no. 7, pp. 1019–1028, 2001.

[31] A. Bemporad, M. Morari, V. Dua, and E. N. Pistikopoulos, "The explicit linear quadratic regulator for constrained systems," *Automatica*, vol. 38, no. 1, pp. 3–20, 2002.

[32] H. J. Kushner, *Stochastic Stability and Control*. Academic Press, 1967.

[33] G. Betti, M. Farina, and R. Scattolini, "Realization issues, tuning, and testing of a distributed predictive control algorithm," *Journal of Process Control*, vol. 24, no. 4, pp. 424–434, 2014.

Irene Perez-Salesa (Graduate Student Member, IEEE) received the B.S. degree in industrial engineering technology and the M.S. degree in industrial engineering from the University of Zaragoza, Zaragoza, Spain, in 2019 and 2021, respectively, where she is currently pursuing the Ph.D. degree in computer science and systems engineering. Her research interests include distributed estimation and control, consensus, and event-triggered communication protocols.

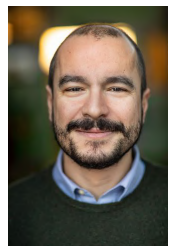

Dimos V. Dimarogonas (Fellow, IEEE) was born in Athens, Greece, in 1978. He received the Diploma degree in electrical and computer engineering and the Ph.D. degree in mechanical engineering from the National Technical University of Athens, Athens, Greece, in 2001 and 2007, respectively. From 2007 to 2010, he was a Postdoctoral Researcher with the Department of Automatic Control, KTH Royal Institute of Technology, Stockholm, Sweden, and the Laboratory for Information and Decision Systems, Massachusetts Institute of Technology, Cambridge, MA, USA. He is currently a Professor with the Division of Decision and Control Systems, School of Electrical Engineering and Computer Science, KTH Royal Institute of Technology. His research interests include multiagent systems, hybrid systems and control, robot navigation and manipulation, human–robot interaction, and networked control. Dr. Dimarogonas is in the Editorial Board of the Automatica and IEEE Transactions on Control of Network Systems. He was a recipient of the ERC Starting Grant in 2014, the ERC Consolidator Grant in 2019, and the Knut och Alice Wallenberg Academy Fellowship in 2015.

Carlos Sagüés (Senior Member, IEEE) received the M.S. degree in computer science and systems engineering and the Ph.D. degree in industrial engineering from the University of Zaragoza, Zaragoza, Spain, in 1989 and 1992, respectively. In 1994, he joined as an Associate Professor with the Departamento de Informática e Ingeniería de Sistemas, University of Zaragoza, where he became a Full Professor in 2009, and was also the Head Teacher. He was engaged in research on force and infrared sensors for robots. His current research interests include control systems and industry applications, computer vision, visual control, and multivehicle cooperative control.

Rodrigo Aldana-López (Member, IEEE) received the B.S. degree in electronics engineering from the Instituto Tecnológico y de Estudios Superiores de Occidente, Tlaquepaque, Mexico, in 2016, and the Ph.D. degree in computer science and systems engineering from the University of Zaragoza, Zaragoza, Spain, in 2024. His research interests include real-time robotics, machine learning, and communication protocols and control for distributed systems.